Non-infectious Parenchymal Lung Disease

G. Dalpiaz and M. Piolanti

Contents

1 **Acute Drug Toxicity** 000
1.1 Introduction 000
1.2 Mechanisms of Injury 000
1.3 Terminology and Clinical Issues 000
1.4 Imaging 000
1.5 Management and Treatment 000

2 **Hypersensitivity Pneumonitis (HP)** 000
2.1 Introduction 000
2.2 Mechanisms of Injury and Causes 000
2.3 Terminology and Clinical Issues 000
2.4 Imaging 000
2.5 Differential Diagnosis 000
2.6 Management and Treatment 000

3 **ARDS** 000
3.1 Introduction 000
3.2 Mechanisms of Injury 000
3.3 Terminology and Clinical Issues 000
3.4 Imaging 000
3.5 Differential Diagnosis 000
3.6 Management and Treatment 000

4 **Diffuse Alveolar Hemorrhage (DAH)** 000
4.1 Introduction 000
4.2 Mechanisms of Injury and Causes 000
4.3 Terminology and Clinical Issues 000
4.4 Imaging 000
4.5 Differential Diagnosis 000
4.6 Management and Treatment 000

5 **Fat Embolism Syndrome (FES)** 000
5.1 Introduction 000
5.2 Mechanisms of Injury 000
5.3 Terminology and Clinical Issues 000
5.4 Imaging 000
5.5 Differential Diagnosis 000
5.6 Management and Treatment 000

6 **Acute Pulmonary Edema** 000
6.1 Introduction 000
6.2 Mechanisms of Injury 000
6.3 Terminology and Clinical Issues 000
6.4 Imaging 000
6.5 Differential Diagnosis 000
6.6 Management and Treatment 000

References 000

Abstract

Acute dyspnea is a common presenting complaint in the emergency room, emergency medicine and intensive care. It may have a cardiovascular or a non-cardiovascular origin, the latter including pulmonary parenchymal diseases. Depending on the cause, it may be associated with fever, cough, hemoptysis, and/or chest pain, with a duration of symptoms that can range from hours to days.

Prompt identification of the underlying cause of acute dyspnea is essential in guiding appropriate therapy and management, as patients may rapidly progress to acute respiratory failure. Evaluation with chest radiography is vital for initial assessment and may

G. Dalpiaz, MD
Radiologia Ospedale Bellaria, AUSL Bologna, Italy
e-mail: giorgia.dalpiaz@ausl.bologna.it

M. Piolanti, MD (✉)
Radiologia Ospedale Maggiore, AUSL Bologna, Italy
e-mail: marco.piolanti@ausl.bo.it

Med Radiol Diagn Imaging (2016)
DOI 10.1007/174_2016_30, © Springer International Publishing Switzerland

reveal diffuse parenchymal abnormalities, which may require further assessment with computed tomography (HRCT).

Acute non-infectious parenchymal lung diseases are often overlooked and may be under-diagnosed. Their diagnosis requires the evaluation, along with the HRCT pattern, of the clinical and laboratory features and of the bronchoalveolar lavage. Biopsy may be necessary in more complex cases.

Although the most frequent cause of diffuse non-infectious parenchymal lung involvement is acute hydrostatic pulmonary edema, there is a wide variety of diseases that may be encountered, including acute drug toxicity, hypersensitivity pneumonitis (HP), acute respiratory distress syndrome (ARDS) and diffuse alveolar hemorrhage (DAH). In trauma patients, fat embolism syndrome (FES) must be taken into account. Acute respiratory failure is an eventuality that can occur during the course of chronic lung diseases (UIP for example), which may have been unknown until then.

1 Acute Drug Toxicity

1.1 Introduction

Drug toxicity is a common condition, often underdiagnosed. As a result, the incidence and the prevalence are underestimated. There are numerous agents with potential toxic effects on the lungs including cytotoxic and noncytotoxic drugs. Common causes of drug-induced lung disease include chemotherapeutic agents, amiodarone, antibiotics, and nonsteroidal anti-inflammatory drugs. There are a number of recognized cofactors that may enhance the likelihood of a pulmonary drug reaction, particularly reactions associated with chemotherapeutic agents. These include advanced age, prior radiotherapy, and elevated inspired oxygen levels; the presence of any or all of these factors increases the likelihood of developing a pulmonary drug reaction. Surgery may even be a precipitating event (Camus et al. 2004a).

1.2 Mechanisms of Injury

Generally, pulmonary drug reactions are the result of either direct or indirect effects of the drug. Reactions due to direct effects can be broadly divided into those that are toxic reactions (which to some extent are dose-related, such as reactions to chemotherapeutic agents) and those that are idiosyncratic reactions (which tend not to show a consistent dose-response relationship). This division is artificial and the distinction between toxic reactions and idiosyncratic reactions is not always clear cut. Several risk and exacerbating factors for diffuse lung disease have been identified. Some of them include advanced age (60 years or older) and existing pulmonary lesions (Kubo et al. 2013).

1.3 Terminology and Clinical Issues

The symptoms may be acute/subacute/chronic and are nonspecific and therefore the diagnosis requires a high index of suspicion by clinician and the radiologist. Acute respiratory failure due to drug-associated ILD generally has an unpredictable onset and rapid time course (onset of clinical manifestations within minutes to hours of taking the drug). Patients with acute drug toxicity present with the progressive or rapid onset of dry cough, high fever, and dyspnea. These patients often require admission to the intensive care unit and mechanical ventilation (Prasad et al. 2014; Camus et al. 2004b).

The identification of drug-induced lung disease requires an active consideration of any change in the patient's clinical course as a possible response to medications. There are no pathognomonic signs, symptoms, laboratory tests, or pathologic features that identify a drug as the cause of the illness. Further, drug-induced lung disease must be distinguished from more common illnesses or causes of acute exacerbation of an ongoing illness such as asthma, infection, congestive heart failure, and pulmonary thromboembolism. A history of drug exposure and a consistent radiological pattern may be diagnostic tools.

Bronchoalveolar lavage (BAL) is particularly helpful in ruling out infectious mostly before

Table 1 Acute drug toxicity: main clinical-histopathologic patterns

Acute clinical-histopathologic patterns	Typical drugs
Diffuse alveolar damage (DAD/ARDS)	Bleomycin, busulfan, cyclophosphamide, mitomycin, amiodarone
Diffuse alveolar hemorrhage (DAH)	Anticoagulants, amphotericin B, cytarabine (ara-C), penicillamine, cyclophosphamide
Pulmonary edema (PE)	Blood transfusions, tricyclic antidepressants, illicit drugs
Hypersensitivity pneumonia (HP)	Methotrexate, cyclophosphamide, nitrofurantoin

corticosteroid therapy. Biopsy can generally be avoided, as it does not always provide a specific diagnosis. Open lung biopsy is rarely performed (Müller et al. 2004).

1.4 Imaging

Several clinical-histopathologic patterns of drug toxicity with acute respiratory failure have been observed (Table 1). The HRCT features of drug-induced lung disease often reflect the histopathologic patterns of reaction (Rossi et al. 2000; Cleverley et al. 2002; Erasmus et al. 2002; Torrisi et al. 2011). For the clinical aspects and imaging of each acute clinical-histopathologic pattern listed in Table 1, we suggest to refer to the other diseases covered in this chapter. A new and continuously updated website is available for information on drug-induced pulmonary reactions: http://www.pneumotox.com.

1.5 Management and Treatment

Disease types such as pulmonary edema and hypersensitivity pneumonia generally have a favorable clinical course and most patients resolve following drug discontinuation or treatment with corticosteroids. In contrast, DAD rarely responds to treatment and has a poor prognosis, and even if it resolves, fibrosis may remain as a sequela.

2 Hypersensitivity Pneumonitis (HP)

2.1 Introduction

Hypersensitivity pneumonitis (HP), also known as extrinsic allergic alveolitis, is a syndrome that results from repeated inhalation and subsequent sensitization to a wide variety of airborne organic particles. The presentation and clinical course are highly variable and depend from intensity and duration of exposure to the antigen and the nature of the antigen and specific factors of the host, such as an individual predisposition probably genetically determined (Spagnolo et al. 2015). According to data from registries of interstitial lung diseases (ILDs) in three European countries, HP accounts for 4–15 % of all ILD cases (Thomeer et al. 2001). However, the incidence and prevalence of HP are difficult to estimate with precision, mainly because of the number of cases that are misdiagnosed or not recognized and a lack of uniform diagnostic criteria.

The disease is diagnosed on the basis of a history of exposure to an offending antigen with onset of compatible clinical, HRCT, or physiological findings within 4–12 h. Other diagnostic criteria include clinical improvement after removal from exposure and recurrence on reexposure. In cases where the inciting antigen cannot be identified or in the presence of conflicting clinical, radiological, and functional findings, fiberoptic bronchoscopy with bronchoalveolar lavage (BAL) and transbronchial lung biopsy are indicated. Surgical lung biopsy is only required if these prove inconclusive (Elicker et al. 2016).

2.2 Mechanisms of Injury and Causes

HP comes from an immune-mediated inflammatory process involving the lung parenchyma (terminal bronchioles, alveoli, and interstitium), based on mechanisms likely independent from single causative agent, mediated by immune complexes in the acute phases of the disease and an altered response of T lymphocytes in the early stages subacute and

Table 2 Major classes of antigens and corresponding types of hypersensitivity pneumonitis

Class of antigens	Specific antigens	Disease prototypes
Fungi	*Aspergillus*	Farmer's lung Mushrooms worker's lung
Mycobacteria	*Mycobacterium avium-intracellulare*	Hot tub lung Swimming pool lung
Bacteria	*Saccharopolyspora rectivirgula*	Farmer's lung
Animal proteins	*Avian proteins*	Bird fancier's lung
	Silkworm proteins	Silk production HP
Chemicals	*Diisocyanates, trimellitic anhydride*	Chemical worker's lung

chronic (Vogelmeier et al. 1993; Barrera et al. 2008). HP seems that cigarette smoking can play a protective effect by reducing the intensity of hyperimmune response. The immune pathogenesis, not yet fully clarified, is linked to hyperactivity of T cells and the action of immune complexes.

In every living environment, antigens potentially causative of the disease may be present. The reported culprits have included microbes, animal and plant proteins, and low-molecular-weight chemicals that combine with host proteins to form haptens. HP-inducing antigens may be classified in broad categories represented by disease prototypes (Table 2) (Hanak et al. 2007; Spagnolo et al. 2015; Selman 2011). In the table is a selected list of the possible innumerable agents and disease.

2.3 Terminology and Clinical Issues

HP has been conventionally classified as acute, subacute, and chronic (Richerson et al. 1989), although a significant overlap exists and there are no widely accepted criteria to distinguish the various forms. In this regard, (Selman et al. 2012) proposed an alternative classification scheme based primarily on disease behavior, distinguishing between acute nonprogressive and intermittent disease, acute progressive/subacute disease, chronic nonprogressive disease, and chronic progressive disease. Which pattern of illness occurs presumably depends upon the intensity and duration of contact, the nature of the antigen, and host factors.

Acute HP is characterized by an influenza-like syndrome occurring a few hours after a substantial exposure. Symptoms gradually decrease over hours/days but often recur with reexposure. Acute episodes can be indistinguishable from an acute respiratory infection caused by viral or mycoplasmal agents. Attacks often follow exposure to the allergen within enclosed spaces with poor ventilation. Patients typically have a restrictive ventilatory defect with reduced DLCO or, in rare cases, an obstructive pattern. Mild hypoxemia at rest is common. In general, the acute form is nonprogressive and intermittent, with spontaneous improvement after antigen avoidance (Selman et al. 2012).

2.4 Imaging

2.4.1 Radiological Signs

Chest radiograph may be normal. Abnormal radiographic findings observed in some patients include a variable combination of fine nodular opacities and widespread ground-glass opacity or, more rarely, as consolidation. The zonal distribution varies from patient to patient and may vary over time in the same patient (Unger et al. 1973; Mönkäre et al. 1985).

2.4.2 CT Signs

High-resolution CT has greatly improved the radiological diagnosis of hypersensitivity pneumonitis because it is more sensitive and specific than chest X-ray. HRCT may either show typical findings, which may be virtually diagnostic of HP in the appropriate clinical setting, or provide important clues that may suggest a correct diagnosis.

HRCT findings vary widely based on the stages of the disease. Only a few reports have described HRCT abnormalities in acute HP, as HRCT is seldom performed at this stage due to the rapid resolution of symptoms. However, in cases with severe clinical manifestations

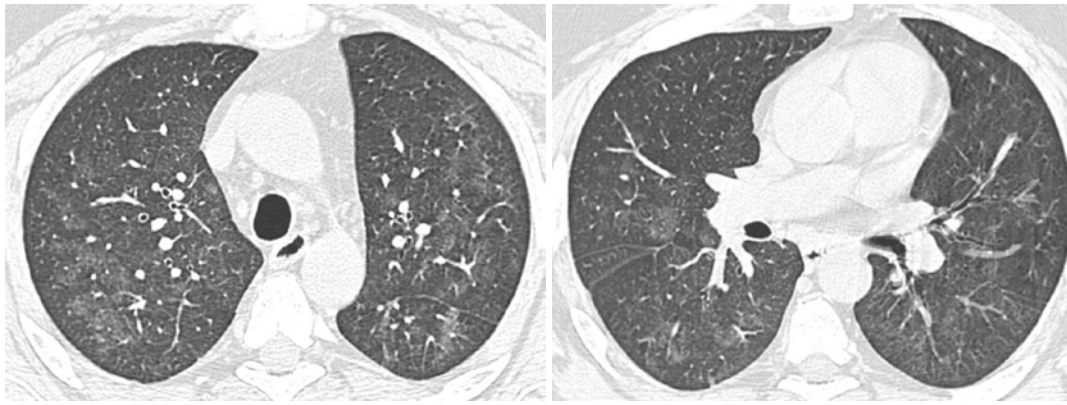

Fig. 1 Hypersensitivity pneumonitis with acute onset. High-resolution computed tomography showing diffuse ground-glass opacity, which is bilateral and symmetric

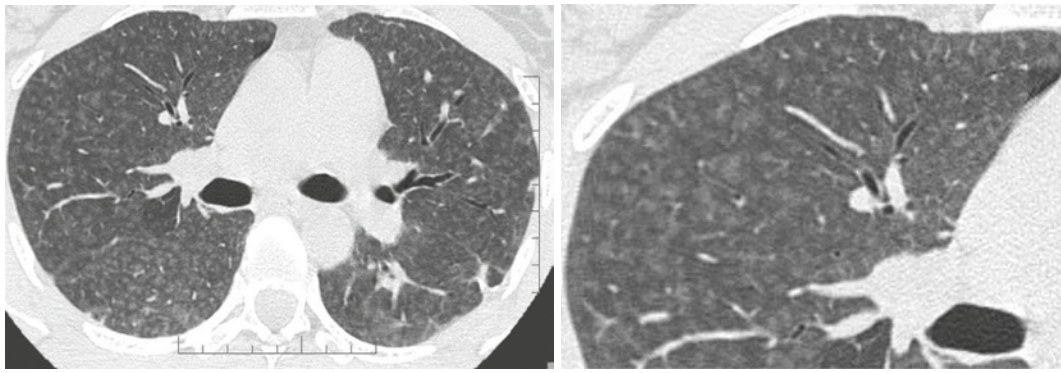

Fig. 2 Hypersensitivity pneumonitis. Axial high-resolution CT images depict bilateral and numerous centrilobular nodules with low-density and ill-defined margins. In terms of their aspect, the nodules are similar to snowflakes. The nodules are diffuse with uniform distribution. *Dark areas* of lobular size due to air trapping are also visible

(e.g., acute respiratory failure), acute HP on HRCT scans may resemble the exudative phase of diffuse alveolar damage (DAD) (Schwarz and Albert 2004). Diffuse ground-glass opacity is usually bilateral and symmetric but sometimes patchy and concentrated in the middle part and base of the lungs (Cormier et al. 2000; Zompatori et al. 2003) (Fig. 1). Furthermore, ground-glass opacity (GGO) superimposed on a background of chronic changes may be observed in acute exacerbation of chronic HP or in chronic cases following intense exposure to antigens.

HRCT abnormalities observed in the subacute phase of the disease may be more specific and include numerous poorly defined nodules, GGO, and areas of decreased attenuation. The nodules with low-density and ill-defined margins usually present less than 5 mm in diameter (also defined centrilobular ground-glass opacities). In terms of their aspect, the nodules are similar to snowflakes. Poorly defined nodules may be the predominant (Fig. 2) or only associated abnormality in patients with subacute HP. These abnormalities represent cellular bronchiolitis, peribronchiolar interstitial inflammation, or, less frequently, focal organizing pneumonia (Maffessanti and Dalpaz 2011).

The key sign to the diagnosis is the coexistence of sporadic lobular areas of air trapping appearing as patches of black lung (Fig. 3). These regions of lobular air trapping are caused by concomitant bronchiolar inflammation and obstruction.

Thus, the combination of a ground-glass opacification, lobular air trapping, and centrilobular

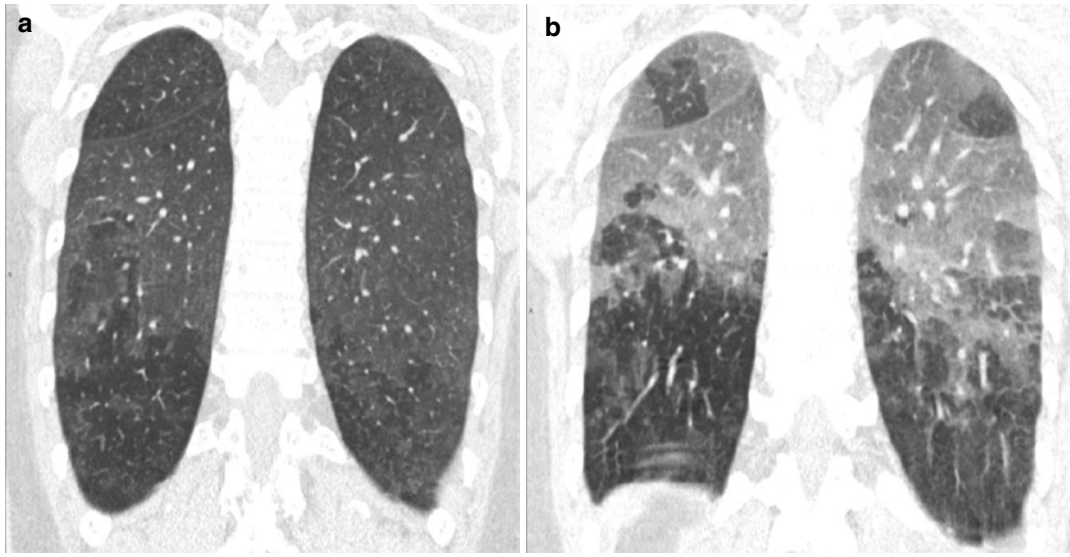

Fig. 3 Recurrent bird fancier's disease. (**a**) Coronal reformatted computed tomography (CT) image obtained at suspended inspiration demonstrates patchy ground glass involving the medium-upper zones combined with areas of decreased attenuation. (**b**) The intensity of the areas of decreased attenuation increases on expiratory CT indicating small airway involvement, an almost invariable finding in hypersensitivity pneumonitis. A few *dark areas* of lobular size due to air trapping are visible in the upper lobes

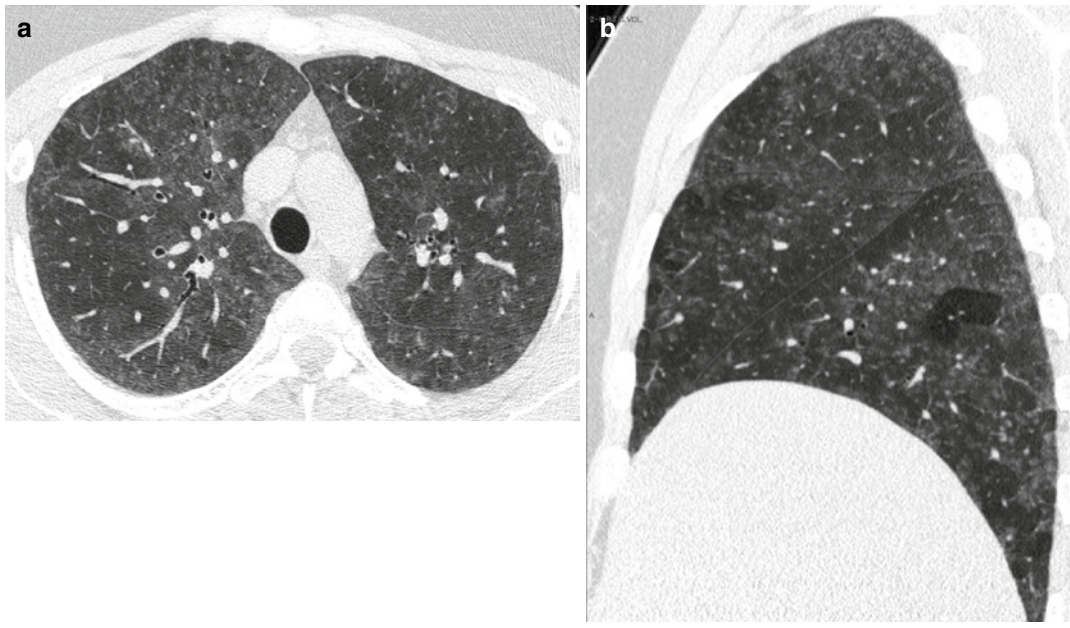

Fig. 4 (**a**, **b**) Typical high-resolution CT abnormalities in patients with hypersensitivity pneumonitis with insidious course and recurrent acute exacerbation include ground-glass opacity, air trapping, and centrilobular ground-glass opacities

nodules is particularly suggestive of acute and insidious onset without fibrosis (Fig. 4) (Silva et al. 2007).

The variable combination of areas of decreased attenuation, ground-glass opacities, and normal lung may produce the so-called

head-cheese pattern, which is highly suggestive of HP (Chong et al. 2014). Coexisting thin-walled lung cysts have been reported in 13 % of patients with subacute HP (Franquet et al. 2003) and are believed to be caused by partial bronchiolar obstruction by peribronchiolar lymphocytic infiltration. These cysts are usually few in number and range in size from 3 to 25 mm. Occasionally in patients with an insidious onset of disease, focal consolidation is present, presumably representing organizing pneumonia. Mediastinal lymph node enlargement has been described in approximately 30 % of patients.

2.5 Differential Diagnosis

The differential diagnosis with other disorders manifesting with acute/subacute diffuse GGO e.g., opportunistic infections, pulmonary edema, and cellular nonspecific interstitial pneumonia (NSIP) may be difficult. However in HP the frequent association of lobular air trapping and centrilobular snowflake nodules is crucial for the diagnosis.

The so-called head-cheese pattern may also be observed in respiratory bronchiolitis-associated ILD (RB-ILD). Integrating nicotine poisoning and laboratory findings may indicate the most likely diagnosis (Chong et al. 2014).

GGO combined with cysts resemble those seen in lymphocytic interstitial pneumonia (LIP). However, LIP is often associated with other conditions, such as connective tissue diseases or lymphatic disorders (e.g., human immunodeficiency virus infection, lymphoma) (Ichikawa et al. 1994).

2.6 Management and Treatment

Patients with acute/subacute HP, if correctly and timely diagnosed and treated, generally have an excellent prognosis. The most important recommended therapy is inhibiting exposure to the causal agent by eliminating it from the environment, avoiding settings where it is present, or using a respirator in those settings. Systemic corticosteroids for a few days to weeks may improve symptoms. Indications for the use of such drugs include acute, severe, or progressive disease (Kokkarinen et al. 1992).

3 ARDS

3.1 Introduction

Acute respiratory distress syndrome (ARDS) is a condition characterized by sudden onset of severe hypoxemia and diffuse pulmonary infiltrates.

The syndrome was firstly introduced by Ashbaugh and colleagues in 1967 (Ashbaugh et al. 1967), while the criteria for the diagnosis of ARDS were first established in 1994 by the American-European Consensus Conference (AECC) (Bernard et al. 1994).

In 2012 the "Berlin definition," the new updated consensus definition of ARDS, has been published in a high-impact journal. ARDS is defined as: "[…] type of acute diffuse, inflammatory lung injury, leading to increased pulmonary vascular permeability, increased lung weight, and loss of aerated lung tissue. The clinical hallmarks are hypoxemia and bilateral radiographic opacities […]" (ARDS Definition Task Force 2012).

3.2 Mechanisms of Injury

ARDS may follow several different types of lung injury that ultimately determine the same monomorphic pulmonary response, characterized histopathologically by the presence of diffuse alveolar damage (DAD).

There are many triggering events that have been classically classified as pulmonary or extrapulmonary. Pulmonary or direct injuries are processes determining direct injury to lungs, like infection, gastric aspiration, or toxic inhalation. Extrapulmonary or indirect injuries may be systemic processes like polytrauma, drug toxicity, sepsis, transfusions, or extra-thoracic diseases like acute pancreatitis.

From a histopathologic point of view, "diffuse" refers to the involvement of the whole alveolar structure: endothelium, basal membrane, and epithelium. The process is widespread throughout

the lungs, but not always in a homogeneous manner: frequently there is presence of spared areas (Kligerman et al. 2013).

The process is characterized by a sequence of phases. Not necessarily the process develops through all the phases: it can stop and reverse anytime (Castro 2006).

The early or exudative phase lasts up to 7 days and is characterized by the presence of hyaline membranes. The alveolar epithelium is damaged and the basal membrane is exposed.

The next stage is the organizing, or proliferative, phase, characterized by the presence of organizing tissue and fibrosis. If this phase does not resolve favorably, there is progression to the last phase, the fibrotic phase.

The pattern of fibrosis is atypical and usually with predilection of the anterior segments (anti-gravitational distribution). Some patients may show areas of "honeycombing," more frequently encountered following acute interstitial pneumonia (AIP), which is the "idiopathic" form ARDS (Tomiyama et al. 2001).

3.3 Terminology and Clinical Issues

The term ARDS should not be confused with the term permeability edema and it is not interchangeable with the term noncardiogenic edema. ARDS is the most severe form of permeability edema, but there are other forms of permeability edema without DAD (Ketai and Godwin 1998). Classification of pulmonary edema is discussed in the "Acute pulmonary edema" section.

ARDS, which is a life-threatening condition, is associated histopathologically to DAD.

In the AECC definition, ARDS was defined as an acute onset of hypoxemia, without specifying a timeframe to define acute; the PaO_2/FiO_2 (ratio of partial pressure of arterial oxygen to fraction of inspired oxygen) must be under <200 mmHg, with presence of bilateral infiltrates on frontal chest X-ray. Presence of left atrial hypertension must be ruled out. PaO_2/FiO_2 between 200 and 300 is termed acute lung injury (ALI).

When idiopathic, the process is termed acute interstitial pneumonia (AIP), also known as Hamman-Rich syndrome (Kliegerman et al. 2013). AIP may sometimes present with a more subacute course, and as a result, it does not always fulfill the criteria of ARDS (Janz et al. 2000).

The new definition of Berlin introduces several important changes to the old criteria (ARDS Definition Task Force 2012). The timeframe for define acute onset is specified within a week from a determinate event. A minimum level of positive end-expiratory pressure (PEEP) is established to evaluate the severity of the respiratory failure. The need to measure pulmonary wedge pressure is removed and the term ALI is suppressed. ARDS is now classified in three grades: mild (200< PaO_2/FiO_2 <300 with PEEP or C-PAP >5 cm H_2O), moderate (100< PaO_2/FiO_2 <200 with PEEP >5 cm H_2O), and severe (PaO_2/FiO_2 <100 with PEEP >5 cmH_2O). Finally, it is stated that the pathologic correlate of ARDS is DAD.

A set of training radiograph is attached to improve interobserver reliability (Ferguson et al. 2012). Opacities seen on CT scan may substitute chest X-ray evaluation for the diagnosis of diffuse pulmonary infiltrates (Table 3).

3.4 Imaging

3.4.1 Radiological Signs

The chest X-ray picture of ARDS varies depending on the phase of the process (Sheard et al. 2012).

In the early or exudative phase, there is some degree of clinical-radiological dissociation, with a latent period after the injury of about 24 h, when the radiograph results normal (Fig. 5a).

Subsequently the appearance of radiographic changes is rapid. The opacification is diffuse and symmetric, peripheral, and with presence of air-bronchograms. The heart and the vascular pedicle are not enlarged; pleural effusion is absent or limited (Fig. 5b). Septal thickening and peribronchial cuffing are less common than in HPE.

The picture remains stable for some days, or longer, during the proliferative phase. In more severe cases, the opacification is complete and

Table 3 Diagnostic criteria for ARDS according to the American-European Consensus Conference (AECC) (Bernard et al. 1994) and to the Berlin definition (ARDS Definition Task Force 2012)

	AECC 1994	Berlin 2012
Onset	"Acute" (no specific timeframe)	Acute "within 7 days of a known clinical insult"
Radiological criteria	Bilateral infiltrates on frontal CXR	"Bilateral infiltrates on frontal CXR not fully explained by effusions, lobar/lung collapse, or nodules /masses" (chest X-ray interpretation set available online)
CT	Not included	Bilateral opacities on CT
Pulmonary artery wedge pressure (PAWP)	PAWP <18 mmHg	Removed
Severity	Acute lung injury (ALI) if PaO_2/FiO_2 <300 (regardless of PEEP level) ARDS PaO_2/FiO_2 < 200 (regardless of PEEP level)	ALI removed Mild/moderate/severe ARDS Minimum C-PAP/PEEP level 5 cmH_2O
Pathologic correlate	Injury to both the epithelium and the endothelium	DAD (diffuse alveolar damage)

the picture is that of the so-called "white lungs" (Fig. 5d, e).

In the late phase the alterations begin to reverse. In patients who heal, the lungs return normal (Fig. 5f), while in patients who develop fibrosis, there is evidence of coarse reticular opacities.

3.4.2 HRCT Signs

The HRCT pattern of ARDS depends on the phase of the process, even if we cannot clearly distinguish the phases. In particular, the exudative phase and the early organizing phase of ARDS overlap, as well as the late proliferative phase overlap with the fibrotic phase (Ichikado 2014).

In the very beginning (early exudative phase), HRCT shows patchy ground-glass opacities (GGO) and consolidations, with geographic distribution (Figs. 5c and 6b). Small pleural effusions (missed by chest X-ray), septal pattern, and crazy paving can also be seen.

Afterward, the process quickly progress to a more homogeneous opacification of the lungs, which persists for the exudative phase and the organizing phase. At this stage ARDS may show two patterns, named typical and atypical. Originally the typical pattern has been associated with extrapulmonary ARDS, while the atypical was associated with pulmonary ARDS (Goodman et al. 1999). This has not been confirmed by a following study (Desai et al. 2001), and in any case, it is not always possible to attribute a single cause to the insurgence of this syndrome (Desai 2002).

The HRCT pattern of typical ARDS is characterized by the presence of a bilateral symmetric anterior-posterior density gradient (Fig. 6c). The density is lower anteriorly (or may be normal or hyperventilated), while posteriorly the density increases progressively, from a ground-glass opacification to a frank consolidation, in the more dependent regions.

In atypical ARDS there are patchy GGO or consolidations, randomly distributed in dependent and nondependent regions of the lungs, without the symmetric density gradient (Fig. 5c).

In the late proliferative and fibrotic phase, from 38 to 85 % of the patients show fibrotic changes in the parenchyma, characterized by an atypical coarse reticular pattern, with traction bronchiectasis and bronchiolectasis (Fig. 7). Fibrotic alterations are more frequently distributed in the ventral portions of the lungs (Fig. 6e, f). This is considered to be the consequence of the barotrauma caused by prolonged ventilation (Nöbauer-Huhman et al. 2001).

CT predictors of mortality in ARDS are signs of right heart failure, involvement of more than 80 % of the lung parenchyma, and presence of varicoid traction bronchiectasis (Chung et al. 2011).

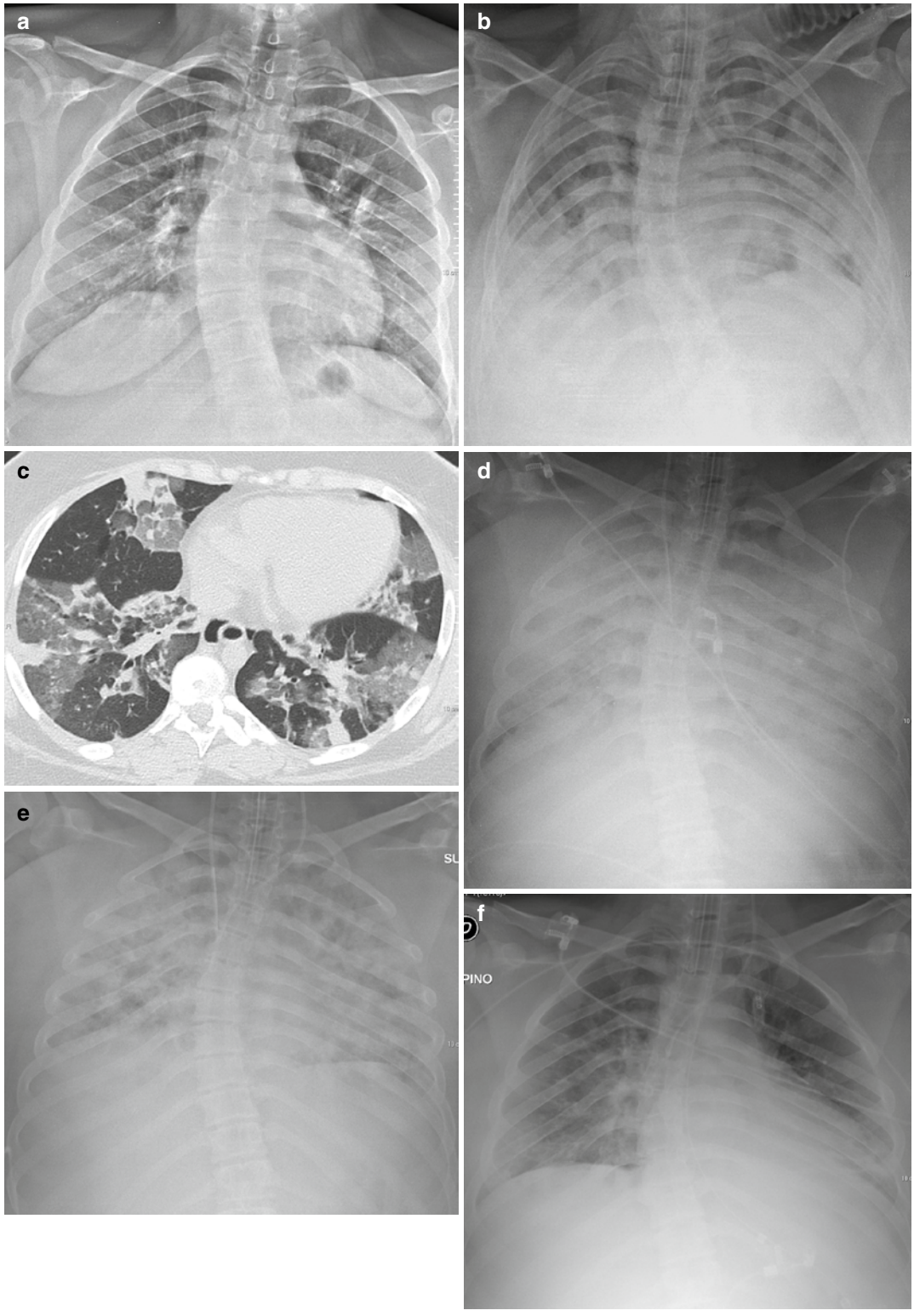
a
b
c
d
e
f

3.5 Differential Diagnosis

Historically, the radiographic differentiation of hydrostatic and permeability edema has always been a big radiological challenge (Milne et al. 1985; Aberle et al. 1988).

Criteria for the radiographic differentiation of permeability edema from hydrostatic pulmonary edema (HPE) have been discussed in the acute pulmonary edema paragraph. Although there are several signs that can help the diagnosis, the distinction is frequently impossible. Moreover, chest radiograph interpretation shows poor interobserver reliability (Rubenfeld et al. 1999; Meade et al. 2000).

Likely HRCT may improve the diagnostic accuracy, but at present there is a scarcity of literature in regard. HRCT findings that suggest presence of HPE are perihilar and upper lobar distribution of GGOs, central predominant distribution of consolidations, dilatation of the pulmonary veins and of the superior cava vein, thickening of the bronchial walls (peribronchovascular thickening), and right pleural effusion. Even distribution of the GGOs and of the consolidations is found more often in ARDS. Gravity-dependent opacities, septal pattern, air bronchograms, and traction bronchiectasis did not show significant difference in prevalence between HPE and ARDS (Komiya et al. 2013).

This difficulty in the differential diagnosis of the nature of the edema is implicitly recognized by the definition of Berlin. In the Berlin definition, a differential diagnosis between cardiogenic and noncardiogenic edema on chest radiograph is not required, nor it is considered relevant: it is now recognized that hydrostatic edema and ARDS may coexist. The diagnosis of ARDS requires that the respiratory failure is not fully explained by cardiac failure, or fluid overload, using all available data (Ferguson et al. 2012). Therefore, radiologically, the focus is on the generic diagnosis of bilateral edema that must not be confused with pleural effusions, lobar/lung collapse, or nodules/masses. In fact, HPE is not the only condition with which the ARDS goes in differential diagnosis: bioptic and autoptic studies have demonstrated only moderate agreement between the clinical diagnosis of ARDS and presence of DAD. Specificity of the various criteria for presence of DAD is variable in literature, but always quite poor (Lorente et al. 2015).

There is no pathognomonic laboratory test or radiological sign to establish the diagnosis of ARDS, which is generally clinical. Apart from HPE, the most common conditions that share a similar clinical presentation are atelectasis, pneumonia, and pulmonary embolism (Murray 1975). In reality there are many more and encountered less frequently: miliary tuberculosis, CMV pneumonia, invasive aspergillosis, hantavirus pneumonia, herpes simplex pneumonia, bronchoalveolar cell carcinoma, drug toxicity, lymphangitis, acute leukemia, lymphoma, veno-occlusive disease, sickle lung, acute eosinophilic pneumonia, acute cryptogenic organizing pneumonia (COP), acute fibrinous organizing pneumonia (AFOP), diffuse alveolar hemorrhage, and acute hypersensitivity pneumonia (Dakin and Griffiths 2002; Schwarz and Albert 2004).

Some of the abovementioned conditions may show peculiar HRCT findings (many are discussed elsewhere in this book). For example, presence of subpleural peripheral distribution of the consolidations is suggestive of acute eosinophilic pneumonia, while peribronchial distribution is suggestive of COP or AFOP (Obadina et al. 2013).

Most of those mimickers (or imitators) of ARDS require a different and specific therapy. Therefore, when performing a HRCT examination in patients with clinical diagnosis of ARDS, maximum attention is required to highlight any

Fig. 5 Evolution of ARDS at chest X-ray (post-infective ARDS). Latent period: no pathologic findings (**a**). The following day appearance of bilateral patchy consolidations, with bilateral pleural effusion (**b**). HRCT, performed on the same day, shows bilateral patchy and lobular GGOs and consolidations, randomly distributed (atypical ARDS) (**c**). The day after, chest X-ray shows bilateral extensive opacification ("lung white-out") (**d**). Parenchymal opacification remains stable: chest X-ray 2 days later (**e**). The patient survived and improved quickly: marked radiographic improvement 7 days later (**f**)

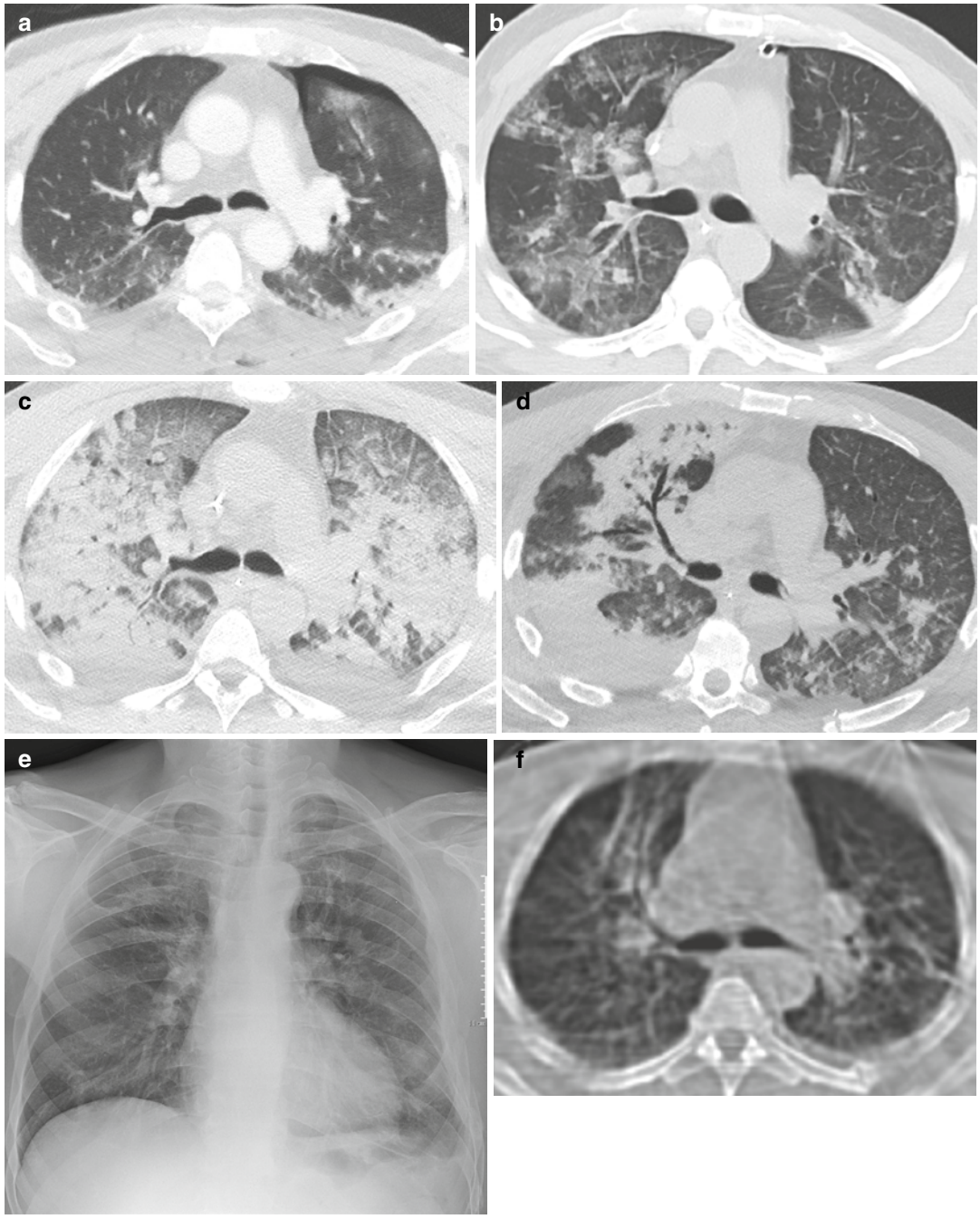

Fig. 6 Evolution of ARDS at CT (posttraumatic ARDS). At admission, left thoracic trauma with pneumothorax and lung contusion (**a**). Respiratory deterioration 7 days later: at CT appearance of bilateral patchy GGO, corresponding to the early exudative phase (**b**). Two days later, extensive lung opacification with extensive dorsal consolidation and ventral GGO: typical ARDS pattern (proliferative or organizative phase). Note presence of smooth septal thickening ("crazy-paving appearance") (**c**). Nine days later advanced regression of the lung opacities: on the right side presence of bronchiectasis and bronchocentric consolidation, located anteriorly (fibro-proliferative phase) (**d**). The patient survived and recovered well, although chest X-ray performed 2 months later demonstrates persistence of coarse fibrosis in the upper right lobe (**e**), confirmed at CT (**f**)

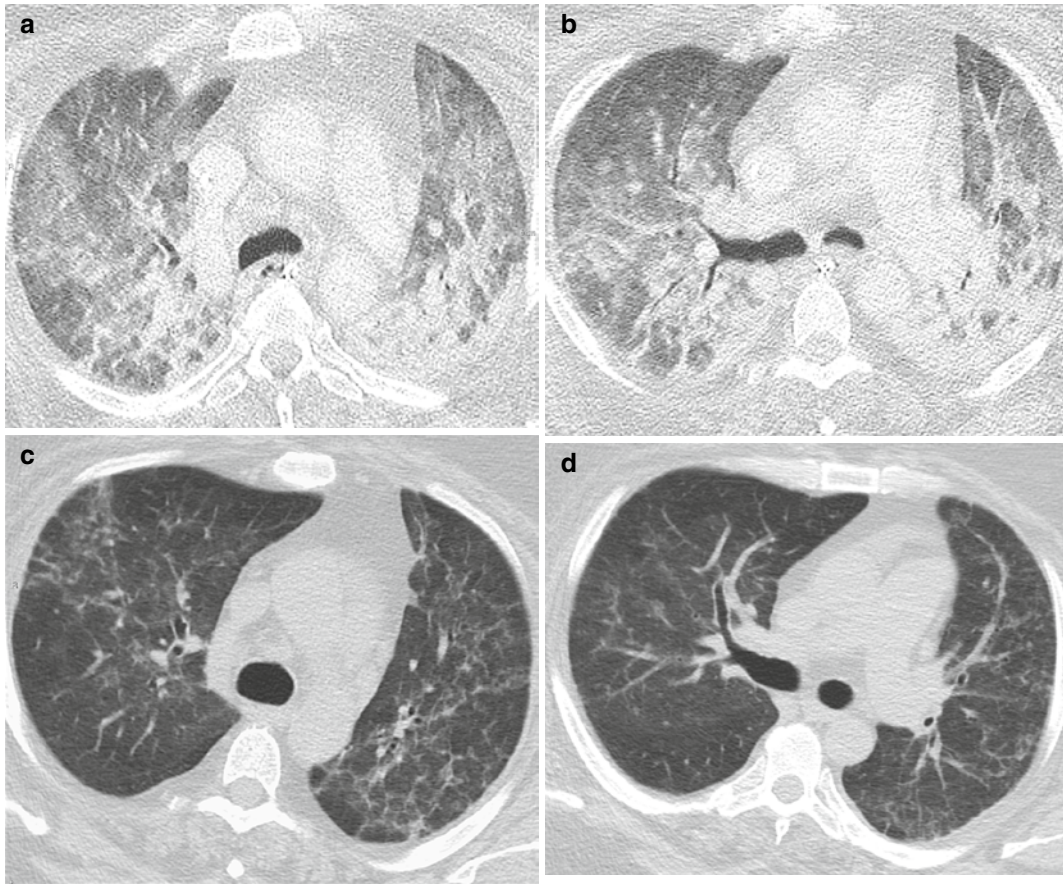

Fig. 7 Severe ARDS followed by fibrotic outcome, caused by viral H1N1 infection. Extensive bilateral consolidations and GGO (**a**, **b**). Two months later, persistence of a reticular pattern bilaterally ("atypical" fibrosis) (**c**, **d**)

sign, or pattern, that may suggest an alternative diagnosis to the complex ARDS/DAD.

3.6 Management and Treatment

No pharmacologic therapy has proved effective in the prevention or management of ARDS.

The only specific therapy for ARDS is ventilation (noninvasive or mechanical) using low tidal volumes (lung-protective strategy), to improve blood oxygen levels, and providing supportive care.

Great deal of attention must be placed to not miss a treatable cause of ARDS and to early diagnose the complications (barotrauma, ventilator-associated pneumonia, and fluid overload, among others).

4 Diffuse Alveolar Hemorrhage (DAH)

4.1 Introduction

Diffuse alveolar hemorrhage (DAH) is not a specific disorder, but a syndrome that suggests a differential diagnosis and a specific sequence of testing. DAH may be a life-threatening condition characterized clinically by the presence of hemoptysis, falling hematocrit, diffuse pulmonary infiltrates, and hypoxemic respiratory failure, which can be severe. However, chest radiographic and CT findings may be nonspecific (the alveolar infiltrates can even sometimes be unilateral), and hemoptysis may be lacking. DAH should be considered a medical

emergency due to the morbidity and mortality associated with failure to treat the disorder promptly (Collard and Schwarz 2004; Lara and Schwarz 2010).

The diagnosis of diffuse alveolar hemorrhage is made on the basis of the clinical and radiological pattern and may be confirmed by bronchoalveolar lavage (BAL). In acute and severe forms, the BAL findings include bright red blood from multiple sites in different bronchi and, microscopically, hemosiderin-laden macrophages. BAL is also useful for excluding other differential diagnoses, such as infections or other endobronchial sources of bleeding (Park 2013). Once the diagnosis is established, the underlying cause must be established in order to initiate treatment.

4.2 Mechanisms of Injury and Causes

DAH is a life-threatening condition which refers to hemorrhage originating in the pulmonary microvasculature, rather than from the bronchial circulation or parenchymal abnormalities. All causes of DAH have the common denominator of an injury to the alveolar microcirculation. Pulmonary small vessel vasculitides, connective tissue disorders, and drugs make up the majority of the cases of DAH (Table 4).

DAH includes diseases associated with pulmonary capillaritis (cellular infiltrate of neutrophils in the capillaries and venules) and those associated with normal vessels (Colby et al. 2001). A pulmonary capillaritis is considered the most common underlying lesion associated with diffuse alveolar hemorrhage.

4.3 Terminology and Clinical Issues

The cardinal sign of DAH, hemoptysis, may be a dramatic event or evolve over days to weeks; however, it may be initially absent in up to 33 % of DAH cases. The other symptoms of DAH are nonspecific and include fever, cough, and dyspnea. Nonpulmonary signs and symptoms are those that accompany the underlying systemic disease. A possible association of hematuria and renal failure due to concomitant glomerulonephritis may be present (Dalpiaz et al. 2003).

The causes of diffuse alveolar hemorrhage are many, but the association with primary renal involvement (pulmonary-renal syndrome) reduces the range of diagnostic possibilities to a handful of diseases: Goodpasture's syndrome, systemic lupus erythematosus (SLE), ANCA-associated vasculitis (antineutrophil cytoplasmic antibodies), particularly micropolyangiitis (MPA), granulomatosis with polyangiitis (Wegener granulomatosis), and, more rarely, eosinophilic granulomatosis with polyangiitis (Churg-Strauss) (Jennette 2013; Chung et al. 2010; Marten et al. 2005; Mayberry et al. 2000). Knowledge of the patient's clinical data and laboratory tests may be sufficient to guide toward the possible cause of this group of patients (Table 5).

Table 4 Causes of diffuse alveolar hemorrhage (DAH)

Main causes of diffuse alveolar hemorrhage
Pulmonary small vessel vasculitides:
ANCA-associated pulmonary vasculitides:
Granulomatosis with polyangiitis (formerly Wegener's granulomatosis)
Microscopic polyangiitis (MPA)
Churg-Strauss vasculitis
Non-ANCA-associated pulmonary vasculitides:
Goodpasture's syndrome
Connective tissue disorders (SLE, mixed connective tissue disease, RA)
Drugs
Other causes of diffuse alveolar hemorrhage
Coagulative disorders
Inhaled toxins
Mitral valve disease
Pulmonary veno-occlusive disease (PVOD)
Infection
Diffuse alveolar damage
Malignancy
Autologous bone marrow transplantation
Acute lung transplant rejection
Pulmonary hemosiderosis
Antiphospholipid syndrome

Table 5 Causes of combination of DAH and glomerulonephritis (primary pulmonary-renal syndrome)

	Clinical features	Laboratory tests
Goodpasture's syndrome	Young man	Anti-GBM
Granulomatosis with polyangiitis (Wegener granulomatosis)	Upper airway disease (nasal, oral, or sinus inflammation)	c-ANCA
Microscopic polyangiitis (MPA)	Systemic symptoms	p-ANCA
Systemic lupus erythematosus (SLE)	Systemic symptoms	ANA
Eosinophilic granulomatosis with polyangiitis (Churg-Strauss)	Asthma	Peripheral eosinophilia p-ANCA

Anti-GBM anti-glomerular basement membrane antibodies, ANCA antineutrophil cytoplasmic autoantibody, *ANA* antinuclear antibodies

Fig. 8 Diffuse alveolar hemorrhage (DAH) in systemic lupus erythematosus (SLE). Chest radiograph shows extensive and patchy parenchymal opacities in both lungs. Both apices and subpleural lungs are relatively spared (bat's wing or butterfly pulmonary opacities)

Fig. 9 Diffuse alveolar hemorrhage (DAH) and alveolar edema in mitral regurgitation resulting from myocardial infarction and papillary muscle rupture. Chest radiograph reveals asymmetrical consolidations predominantly in the right parahilar region

4.4 Imaging

4.4.1 Radiological Signs

The characteristic radiological picture of DAH often shows bilateral parenchymal consolidation or ground-gross opacities, sometimes predominant in the perihilar region ("butterfly wings" or "bat wings" opacities, Fig. 8); occasionally it is prevalently unilateral (Fig. 9) (Primack et al. 1995). The chest radiograph findings are nonspecific and the diagnosis relies combination with clinical and laboratory findings.

4.4.2 CT Signs

High-resolution CT often yields no additional diagnostic information, merely confirming the presence of infiltrates. The HRCT pattern can vary with time of onset of the hemorrhage and the clinical context is crucial in image interpretation.

Acute phase can range from lobular or lobar areas of ground-glass opacities or consolidation or extensive, perihilar (bat's wing or butterfly), or diffuse involvement (Fig. 10a, b) (Cortese et al. 2008; Castañer et al. 2010).

Within days of an acute episode of hemorrhage, interlobular septal thickening may be seen in association with ground-glass opacity (crazy-paving pattern) as hemosiderin-laden macrophages accumulate in the interstitium (Fig. 10c) (Rossi et al. 2003; De Wever et al. 2011).

CT may be useful in the follow-up period, given its ability to demonstrate even the mildest relapse arising after reduction or discontinuation

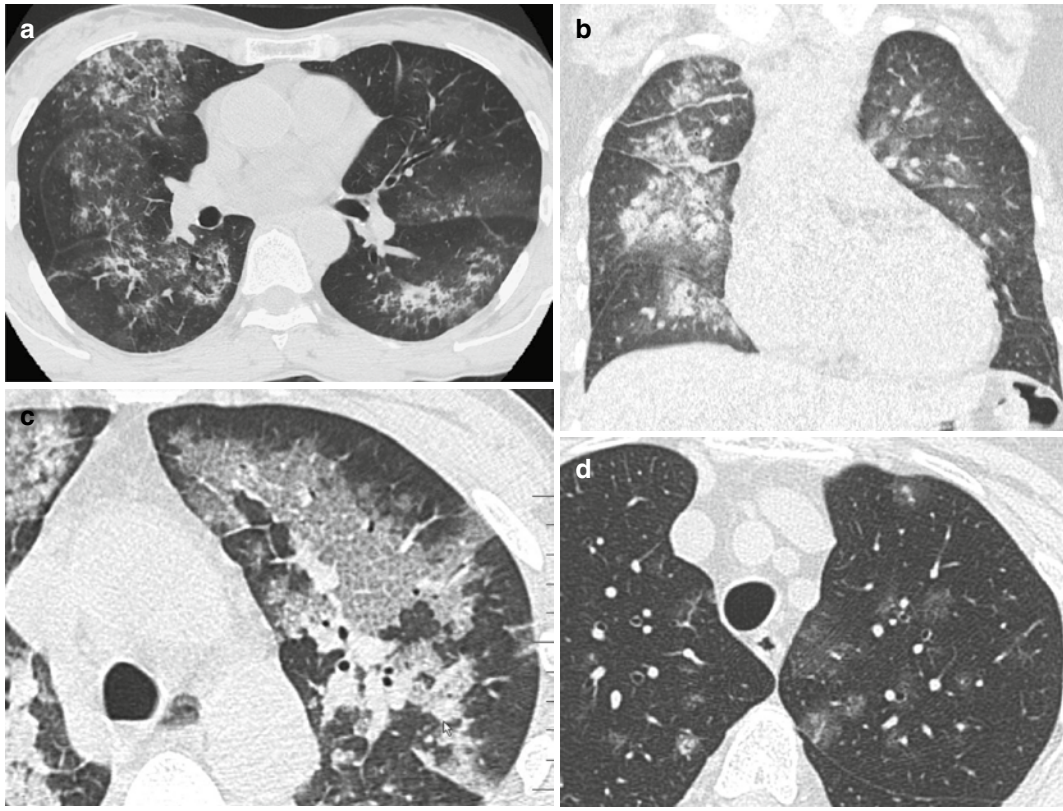

Fig. 10 Variety of high-resolution CT patterns that can be found in DAH. (**a**) Wegener granulomatosis. CT image shows extensive areas of ground-glass opacity in a predominantly perihilar distribution (bat's wing or butterfly pulmonary opacities). (**b**) Mitral regurgitation resulting from myocardial infarction and papillary muscle rupture (same patient as in Fig. 9). CT reveals asymmetrical consolidations and ground-glass opacities predominantly in the right parahilar region. Coexist interstitial edema and enlarged vessels due to concomitant interstitial edema. (**c**) Systemic lupus erythematosus (same patient as in Fig. 8). Within days of an acute episode of hemorrhage, interlobular septal thickening may be seen in association with ground-glass opacity (crazy-paving pattern). (**d**) Microscopic polyangiitis (MPA). CT image shows patchy areas of ground-glass opacity and some low-density nodules (snowflake-like nodules), some of them rounded and feeding-vessels

of cortisone and immunosuppressant therapy. Some faint scattered nodules or small areas of ground glass and some low-density nodules (snowflake-like nodules) may be seen, sometimes around the smaller vessels, which are not detected by chest radiography (Fig. 10d) (Maffessanti et al. 2005).

After repeated episodes of pulmonary hemorrhage, a persistent reticular pattern may be seen, with areas of peripheral traction bronchiectasis and distortion of the lung architecture; this pattern reflects interstitial hemosiderin deposition and mild lung fibrosis and has been termed pulmonary hemosiderosis.

4.5 Differential Diagnosis

Radiological pattern of DHA is not pathognomonic, but diffuse alveolar hemorrhage is the second cause of acute perihilar alveolar lung disease after pulmonary edema (Ribeiro et al. 2006; Dalpiaz and Maffessanti 2013). Differentiation is usually straightforward based on the clinical data and the frequent co-existence, in hydrostatic edema, of pleural effusion, enlarged vessels, and sometimes cardiomegaly. In all these cases, the differential diagnosis with other acute forms of diffuse lung disease—particularly inhalation and infectious pneumonia—based on radiological data alone becomes

impossible. Hemorrhagic alveolar infiltration resolves rapidly (especially after corticosteroid therapy) but slower than pulmonary edema.

4.6 Management and Treatment

The treatment of DAH depends on the underlying cause of hemorrhage and ranges from supportive care and withdrawal of offending drugs to high-dose steroids, immunosuppressants, and plasmapheresis. Massive pulmonary hemorrhage is a life-threatening manifestation and requires aggressive immunosuppressive therapy as soon as possible.

5 Fat Embolism Syndrome (FES)

5.1 Introduction

Fat embolism syndrome (FES) is a rare complication of the fractures, mainly of the long bones. Its importance lies in the fact that it is in the differential diagnosis with other more frequent respiratory complications of trauma and polytrauma, which require a different therapy (such as pulmonary edema or bilateral bronchopneumonia). Also, more rarely, FES can occur in more severe forms such as the acute respiratory distress syndrome (ARDS) or in a fulminant form. While the radiographic findings may be mistaken for other conditions, the CT pattern may be more specific and suggest the diagnosis.

5.2 Mechanisms of Injury

The exact injury mechanism in FES has not been completely explained, nor has the histopathologic picture been completely clarified. The symptomatology has been put in relation to the release of fat particles in the venous blood flow, followed by pulmonary and systemic embolization. At present, it is thought that there are two pathogenic stages that follow one another: the mechanical phase and the biochemical phase (Akhtar 2009). The mechanical phase occurs after release of fat droplets into the venous blood, which determine mechanical obstruction of the pulmonary and systemic capillary bed. The following biochemical phase is due to the toxic effects of free fat acids (FFA) on the endothelia. It is unclear how fat droplets reach systemic circulation: likely they pass through a patent foramen oval or through the pulmonary capillary bed.

Only few studies describe the histopathologic alteration in human FES: in the majority of cases, a toxic vasculitis with alveolar hemorrhage and edema is reported, but also presence of hyaline membranes, the hallmark of diffuse alveolar damage (DAD) and ARDS, has been demonstrated (Berrigan et al. 1966; Dines et al. 1975; Curtis et al. 1979).

Usually fat embolism (FE) is caused by bone fractures, typically by long bone fractures in young patients. Rarely, FE may be due to traumatic subcutaneous fat crushing without fractures (Bolliger et al. 2011) or to nontraumatic causes (Mellor and Soni 2001).

5.3 Terminology and Clinical Issues

Fat embolism (FE) refers to the emergence of fat particles within the venous circulation with the consequent pulmonary embolization. This occurrence is practically constant after fracture, but only a small minority of patients develop clinical symptoms. In those, the resulting syndrome is called fat embolism syndrome (FES) and is characterized by the combination of acute respiratory failure, nervous system impairment, and cutaneous manifestations. The typical petechial rash, that affects the neck, trunk and armpits, characterizes cutaneous manifestations. Petechiae may be evident also in the conjunctiva, retina, or mucosae.

The incidence of posttraumatic FES varies considerably in literature (range from 0.25 % up to 35 %) (Akhtar 2009).

There is no investigation 100 % specific for FES and the syndrome is diagnosed on a clinical base (Mellor and Soni 2001). The most widely accepted diagnostic criteria are those from Gurd and Wilson (Table 6) (Gurd and Wilson 1974).

Table 6 Diagnostic criteria from Gurd and Wilson

Major criteria	Minor criteria
Respiratory insufficiency	Pyrexia
Cerebral involvement	Tachycardia
Petechial rush	Retinal changes
	Anemia
	Thrombocytopenia
	High erythrocyte sedimentation rate
	Fat macroglobulinemia
	Jaundice
	Renal changes

Diagnosis of FES is established when 2 major criteria, or 1 major criterion plus 4 minor criteria, are fulfilled

There are three possible clinical presentation of the fat embolism syndrome. The first is classical response, characterized by transient respiratory failure. It can occur after the trauma or after fixation of the fracture.

The second presentation is with the adult respiratory distress syndrome (ARDS). The third is the so-called hyperacute syndrome: it is extremely rare, is characterized by cardiovascular collapse, and quickly leads to death.

5.4 Imaging

5.4.1 Radiological Signs

Usually the appearance of the radiographic alterations lags behind clinical symptoms, even in already, considerably, symptomatic patients (Fig. 11) (Han et al. 2003).

After an interval (up to 72 h, or even longer), radiographic alterations begin to appear in the perihilar and basal regions. Finally appears the full-blown radiographic picture, which consists of a diffuse interstitio-alveolar involvement, with widespread opacities (Fig. 12). The alterations may be patchy and show relative sparing of the apices (Feldman et al. 1975).

The radiological picture at conventional chest X-ray is considered nonspecific and of little help in the differential from other forms of diffuse airspace disease, like ARDS.

Fig. 11 Early FES. Chest X-ray performed after the onset of the respiratory failure shows poor radiographic alterations

Fig. 12 Full-blown FES. Chest X-ray shows bilateral widespread opacities, with relative sparing of the upper lungs

Sometimes it is possible to identify bilateral focal lesions, described as nodular infiltrates, "rounded densities," or nodular opacities (Fig. 13) (Greenberg 1968; Heyneman and Müller 2000; Arakawa et al. 2000).

Clearing of the radiographic alterations requires a time varying from few days to more than a week (Feldman et al. 1975).

5.4.2 CT Signs

CT findings in pulmonary FES include multifocal ground-glass opacities (GGO) and consolidations, frequently in association with nodules and micronodules. The alterations tend to be bilateral and widespread, with gravitational distribution: consolidations usually have posterior-basal predominance.

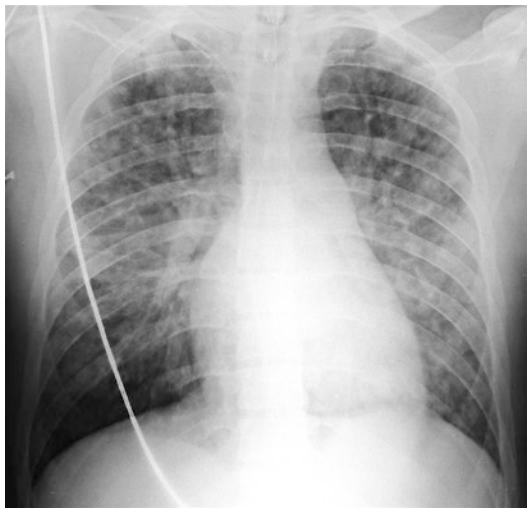

Fig. 13 Nodular pattern as presentation of pulmonary FES. Bilateral nodular and micronodular involvement

The nodules have random distribution, being evident both in the central lobular region and in the subpleural region (Gallardo et al. 2006; Piolanti et al. 2016) (Fig. 14). Also they may present along the interlobular septa (Malagari et al. 2003).

GGO generally have patchy distribution, with geographic appearance (Fig. 15a), and may be frequently associated with septal thickening (Malagari et al. 2003) (Fig. 15b). Consolidations tend to have a gravity-dependent distribution and small pleural effusions are frequent (Arakawa et al. 2000). Consolidations and GGO may present as lobular or sub-lobular opacities (Fig. 14c) (Piolanti et al. 2016).

There are also some case reports of macroscopic fat embolism being detected with contrast-enhanced CT (Ravenel et al. 2002; Nucifora et al. 2007).

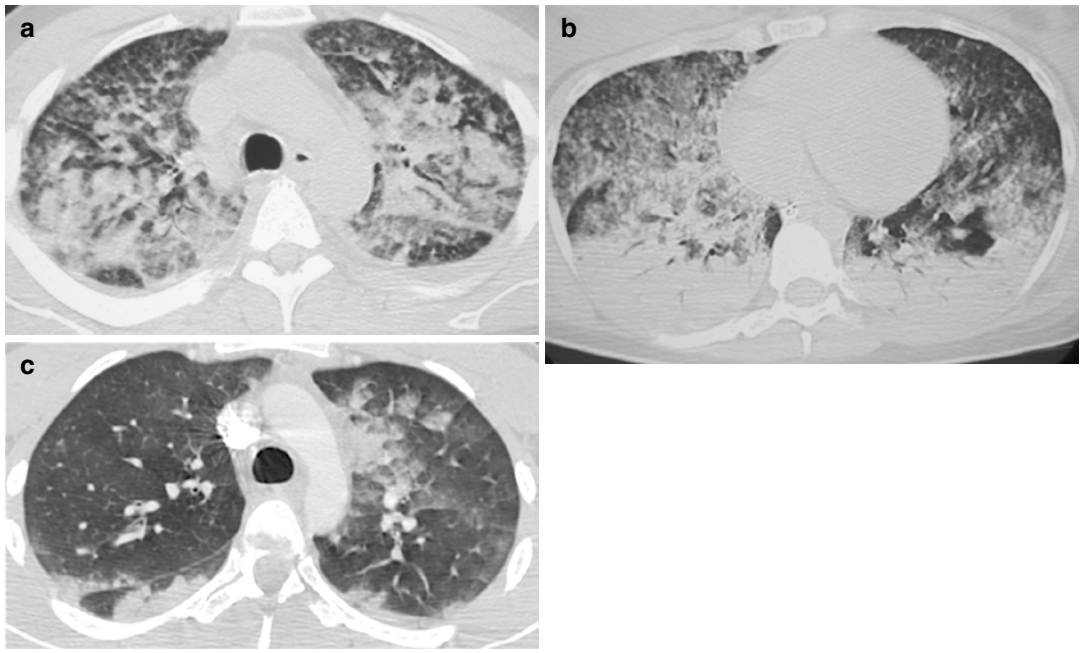

Fig. 14 Nodular pattern at lung CT. Extensive bilateral GGO and consolidations (some showing lobular shape), bilateral nodules, and micronodules: centrilobular and subpleural (randomly distributed) (**a**). Patients with FES and ARDS: anterior-posterior density gradient with dependent consolidations. Presence of an overlapping micro-nodular pattern. (**b**) Lobular and sub-lobular consolidations on the left, subpleural micronodules on the right along the superior fissure (**c**)

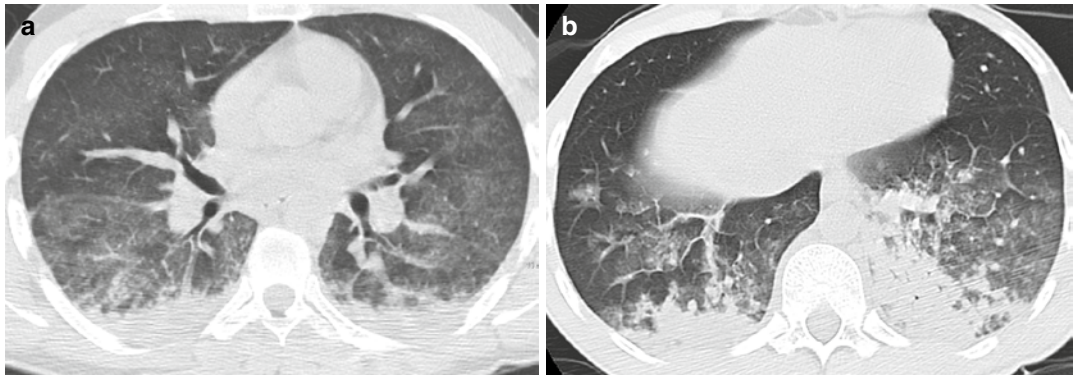

Fig. 15 GGO in acute FES. Diffuse GGO with geographic distribution (**a**). Presence of bilateral smooth interlobular septal thickening. On the right side anterior-posterior density gradient with presence of GGO anteriorly. On the left side GGO are extensive and the overlapping of septal thickening generates a crazy-paving appearance (**b**)

5.5 Differential Diagnosis

Although full-blown or severe FES is not a frequent eventuality, and its frequency is decreasing since early stabilization of the fractures was introduced, it is an important condition to be kept in mind. Its importance lies in the fact that it must be differentiated from other more common and dangerous complications of fractures and polytrauma, such as pulmonary embolism and pneumonia, requiring a specific therapy.

In fact, in the posttraumatic setting, FES has a wide range of conditions from which it must be differentiated: hydrostatic pulmonary edema, fluid overload, neurogenic pulmonary edema, pulmonary contusions, aspiration, viral pneumonia, bilateral bronchopneumonia, ventilator-associated pneumonia, sepsis, ARDS, atelectasis, pulmonary hemorrhage, pulmonary embolism, and drug reactions (Feldman et al. 1975).

Normal heart size, normal vascular distribution, and absence of signs of pulmonary hypertension (Kerley lines, peribronchial cuffing, and widening of the vascular pedicle) are considered findings helpful in differential diagnosis from HPE at chest X-ray (Han et al. 2003). In reality, septal thickening, the equivalent of the Kerley lines at HRCT, is a frequent finding in FES (Malagari et al. 2003).

Lung contusions generally appear at chest X-ray as patchy airspace opacities, unilateral and asymmetric. At HRCT they appear as GGO or consolidations, with ill-defined borders and non-segmental distribution. They may show subpleural sparing. After the trauma they may extend and reach the maximum extension in 24–48 h (Kaewlai et al. 2008; Mirka et al. 2012). This is very helpful in the differential with FES that shows up after a latent period, and its pulmonary alterations are usually bilateral and diffuse.

Viral and bacterial pneumonias may present with several different patterns at CT, with considerable overlap in the imaging appearance (Miller et al. 2011). The presence at HRCT of an "airway- centric" disease, which is characterized by bronchial wall thickening, bronco-centric nodules, lobular opacities, and tree in bud opacities, is highly suggestive of bronchopneumonia (Ketai et al. 2008). Absence of tree in bud opacities and the random distribution of the nodules in FES results to be a useful sign for the differentiation from bronchopneumonia.

Aspiration may show different HRCT patterns: obstruction of the airways by foreign body, tree in bud opacities, or segmental or lobar opacities. Aspiration tends to interest posterior segments of the upper lobes and superior segments of the lower lobes. A massive intake of gastric content causes a severe chemical pneumonia, leading to ARDS (Medelson's syndrome) (Kim et al. 2008).

5.6 Management and Treatment

The treatment of FES is essentially supportive.

Early stabilization of fractures involving the long bones decreases the incidence of FES (Talucci et al. 1983; Svenningsen et al. 1987).

However, it is still unclear what is the best surgical strategy in patients who already show signs of FES. Furthermore, effective pharmacologic therapies have not been found yet, except for steroids. However, their effectiveness has not been proven in prospective studies on a large scale (Akhtar 2009).

6 Acute Pulmonary Edema

6.1 Introduction

Pulmonary edema is defined as presence of excess extravascular fluid in the lungs. The more common type of acute pulmonary edema is hydrostatic pulmonary edema (HPE) due to acute cardiac failure or to fluid overload (overhydration or renal failure).

From a radiological point of view, HPE is the most frequent cause of acute diffuse pulmonary disease (Ketai and Washington 2002).

Chest X-ray is the classical radiological examination for the diagnosis of HPE, while lung sonography is an emerging technique (Cardinale et al. 2014).

CT is not performed for suspected HPE, but HPE is a frequent finding in CT examinations performed for different purposes (e.g., to rule out suspected pulmonary embolism).

6.2 Mechanisms of Injury

The Starling equation describes the factors determining the flow of the fluids between the pulmonary capillary circulation and the lung interstitium (Ware and Matthay 2005). Edema occurs when accumulation of extravascular fluid (transudative or exudative) exceeds the resorption mechanisms (lymphatic absorption). Factors determining the amount of capillary filtration are the transmural hydrostatic pressure, the transmural oncotic pressure, and the permeability of the capillary membrane.

Generally speaking, HPE appears when transmural hydrostatic pressure increases or intravascular oncotic pressure decreases. The fluid is a transudate with low-protein content. The excess of fluid accumulates first in the interstitium and then moves to the pleural and alveolar spaces.

Noncardiogenic edema is due to an increase in permeability of the pulmonary capillaries that allows the outflow of plasma proteins, without increase in transmural hydrostatic pressure. This protein outflow attracts fluids into the interstitial compartment generating an exudative edema, called "permeability edema." In diffuse alveolar damage (DAD), the injury to the endothelial barrier originates the increase in permeability. This is not the sole mechanism of increased capillary permeability that may also occur without DAD, like in cases of reaction to drugs (illicit drugs, interleukin-2 edema), transfusion reaction (classically defined by Milne "allergic lung"), or infection (e.g., hantavirus pulmonary syndrome) (Ketai and Godwin 1998).

6.3 Terminology and Clinical Issues

Acute pulmonary edema is classically classified into cardiogenic and noncardiogenic pulmonary edema.

Cardiogenic pulmonary edema is also referred to as hemodynamic edema or hydrostatic pulmonary edema (HPE). Elevated hydrostatic pressure follows pulmonary venous hypertension, which can be caused by left heart failure or by volume overload (Ware and Matthay 2005).

Noncardiogenic pulmonary edema is also referred to as permeability or injury edema and it is classified into two types: permeability edema with diffuse alveolar damage (DAD) and permeability edema without DAD (Ketai and Godwin 1998).

Finally, edema may be mixed hydrostatic and permeability. A cardiogenic edema may not be purely hydrostatic, since marked elevation of

transmural pressure may generate some degree of epithelial damage, or a volume overload may complicate a permeability edema, generating a mixed edema.

High-altitude, re-expansion, and neurogenic pulmonary edemas are included into the mixed edema group: although their pathogenesis is still incompletely explained, in all cases a hydrostatic component is supposed to combine with some degree of increases in permeability (Ketai and Godwin 1998; Gluecker et al. 1999).

6.4 Imaging

6.4.1 Radiological Signs

Chest radiograph is routinely performed in patients with suspected HPE to confirm the diagnosis or rule out other possible causes. Radiographic findings associated with HPE are increased heart size, increased width of the vascular pedicle, balanced or inverted vascular distribution (redistribution or "cephalization" of the lung vessels), vascular haziness, central or even distribution of the opacities and presence of peribronchial cuffing, septal lines, thickening of the fissures, and pleural effusion.

Radiographically pulmonary edema is divided into three degrees: mild, moderate, and severe (Rubinowitz et al. 2007; Morgan and Goodman 1991).

Mild-degree edema or venous hypertension may show an enlarged vascular pedicle and pulmonary redistribution (cephalization or inversion), which is more frequently seen in cases of chronic heart failure (Fig. 16). Similarly, the heart does not usually enlarge at the first episode of left ventricular failure. Patients with mild edema due to volume overload or to renal failure may show balanced flow, a finding that can be evaluated only in the upright position.

Moderate or interstitial edema shows peribronchial cuffing, Kerley B-lines (septal lines), thickening of the interlobar fissures, and vascular haziness (indistinctness) (Fig. 17).

Severe or alveolar edema shows airspace opacification, prevalent in the middle and lower lung fields (perihilar or gravitational) (Figs. 18 and 19).

Fig. 16 Mild-degree edema or venous hypertension. Pulmonary redistribution, enlarged heart, and enlarged vascular pedicle

Fig. 17 Moderate or interstitial edema. Peribronchial cuffing, bilateral B Kerley lines, thickening of the interlobular fissure, and vascular haziness

The alterations typically are symmetric, but they may be asymmetric in patients with pulmonary parenchymal disease (e.g., emphysema). Unilateral edema is also possible (e.g., in case of mitral cord rupture or of lying on one side) (Fig. 20a, b).

Measurements of the vascular pedicle width can provide an estimate of the intravascular volume status, both in the upright and in the supine position. A vascular pedicle larger than 53 mm in the upright position and more than 70 mm in the supine is

expression of HPE and of fluid overload (Milne and Pistolesi 1994; Ely and Haponik 2002). This measurement may provide evidence of HPE before evidence of clinical signs and help distinguish HPE from permeability edema (Milne 2010).

The radiographic picture is considered to depend from the pulmonary capillary wedge pressure (PCWP), which is an indirect measure of the left atrial pressure: however, in literature, there are great discrepancies and controversies on this topic. With PCWP under 19–25 mmHg, there is equalization or cephalization of the vasculature. Between 20 and 30 mmHg, there is a radiographic picture of interstitial edema. Alveolar flooding appears with over 25–30 mmHg, resulting in the radiological appearance of confluent acinar opacity (Morgan et al. 1991; Ketai and Godwin 1998). It is important to remember how the radiographic picture depends also from the acuteness or chronicity of

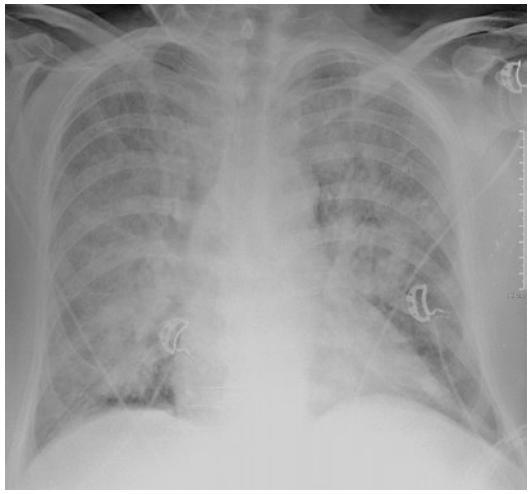

Fig. 18 Severe or alveolar edema. Bilateral airspace opacification, prevalent in the middle or lower fields

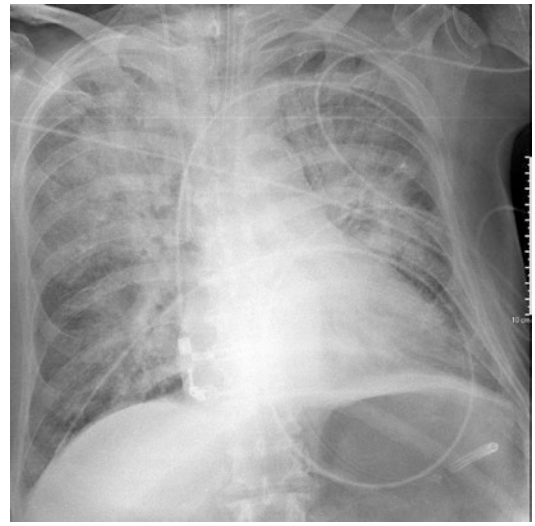

Fig. 19 Alveolar edema with the so-called "bat wings" or "butterfly wings" appearance. Non-gravitational bilateral perihilar opacities with sparing of the lung periphery

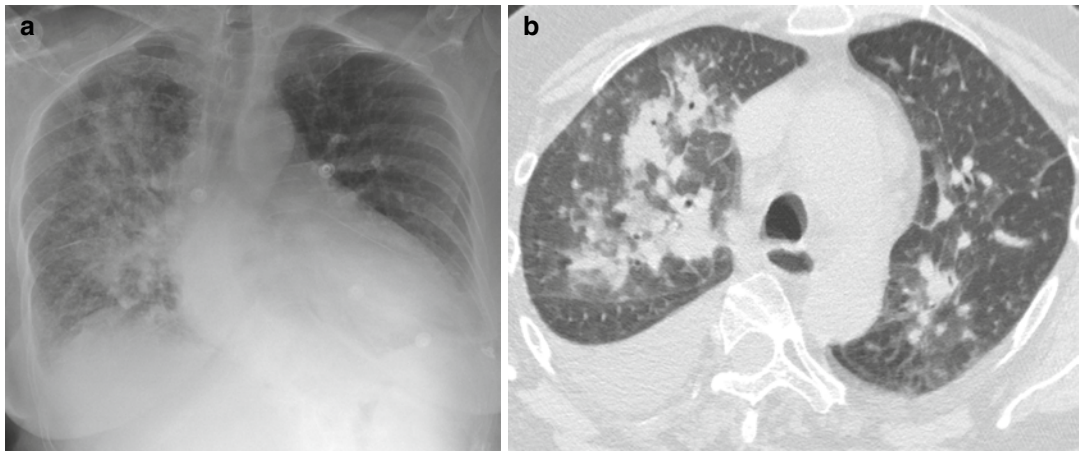

Fig. 20 Unilateral alveolar edema in a patient with acute mitral incompetence (rupture of a papillary muscle). Radiographic picture, extended right-side perihilar opacity, pulmonary redistribution, and enlarged heart (**a**); HRCT findings, presence of right lateral perihilar consolidations; bilaterally smooth septal thickening (septal pattern), bronchial wall thickening, and pleural effusion (**b**)

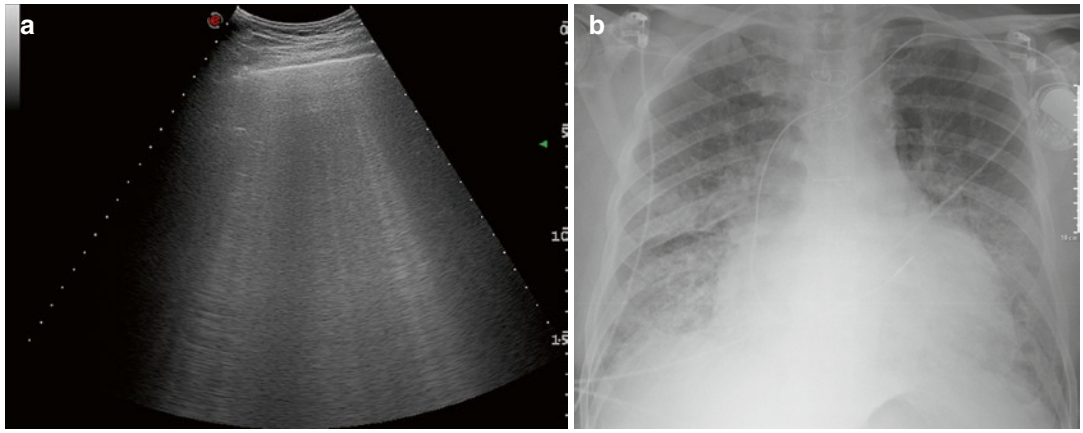

Fig. 21 Lung sonography. Interstitial syndrome characterized by presence of multiple B-lines: left-basal scan (**a**). Corresponding X-ray picture (**b**)

heart failure: edema in acute heart failure is determined by lower pressure gradients, but may not show at chest X-ray dilatation of the heart and of the vessels. On the contrary, chronic heart failure determines an increase in the compliance of the heart and of the pulmonary vessels, and higher pressures are required to determine vascular dilatation (Ketai and Godwin 1998).

Chest X-ray has some intrinsic and technical issues that limit its diagnostic accuracy (Ware and Matthay 2005; Ketai and Godwin 1998). Before radiographic changes start to appear, the water content of the lungs may have to increase up to 30%; alterations may persist up to 24 h after regression of the edema; bedside radiograms obtained with portable X-ray equipment have intrinsically poor technical quality, and they are affected by factors related to the difficulty to optimize the technique of execution, such as positioning of the patient, patients' body weight, degree of inspiration, type of ventilation applied, and focal film distance and exposure; consolidation at chest X-ray is a nonspecific finding, reflecting loss of the air content of the alveoli, and may be subtended by processes other than HPE, such as hemorrhage, pneumonia, inflammation, or tumor.

6.4.2 Lung Sonography

Lung sonography (LUS) is a relatively new and promising technique, based on the evaluation of sonographic artifacts generated by the lungs. In particular, one of them, the so-called B-lines, underlines the so-called interstitial syndrome (Cardinale et al. 2014) (Fig. 21). LUS is highly sensitive in detecting the B-lines, which are vertical echogenic linear artifacts (reverberations).

The interstitial syndrome is a nonspecific finding, which reflects any condition of the lung where alveolar air is partially replaced with increase in interstitial fluids or cellularity. The detection of an interstitial syndrome is not an exclusive feature of HPE and does not allow differentiation of the underlying interstitial disease. Combining the distribution and the number of the B-lines, with other sonographic signs (peripheral consolidations and aspect of the pleural line) and with the physical examination, may allow to differentiate cardiogenic and noncardiogenic causes of the interstitial syndrome (Copetti et al. 2008; Gargani and Volpicelli 2014).

The advantages of ultrasound are the low cost, noninvasiveness, repeatability, the possibility to perform bedside (point-of-care sonography), and the lack of use of ionizing radiation.

This technique is meeting a great enthusiasm on the part of clinicians and researchers. Certainly, in the next few years, researchers and scientific societies will clarify the potentialities, and the role, of this innovative approach.

6.4.3 CT Signs

Lung HRCT is more sensitive in detecting edema findings compared to chest X-ray (Rubinowitz et al. 2007).

Unfortunately, it is too irradiating, and expensive, to be used routinely for the detection of HPE. For this reason, there are no studies that correlate the CT findings with the degree of HPE.

In the clinical practice, HPE is some kind of "incidentaloma," found at a CT examination performed to rule out other diseases (acute pulmonary embolism above all). It is therefore important to readily recognize HPE at CT to address properly the diagnostic and therapeutic procedures.

The main HRCT findings of HPE are septal pattern, or smooth thickening of the interlobular septa, and ground-glass opacities (GGO) (Figs. 22 and 23).

Other findings are bronchial wall thickening (or smooth peribronchovascular interstitial thickening), enlarged vessels, thickening of the fissures, and ill-defined perivascular and centrilobular opacities and consolidations (Storto et al. 1995; Ribeiro et al. 2006).

GGO are typically patchy, may be lobular, or may present as crazy paving.

At CT the distribution of the alterations tends to show parahilar and posterior distribution. HPE may also show up with a gravity-dependent density gradient (Komiya et al. 2013).

6.5 Differential Diagnosis

There are several radiographic signs that may help the differential between HPE and noncardiogenic pulmonary edema (Milne et al. 1985; Aberle et al. 1988).

Typically, cardiogenic pulmonary edema shows cardiomegaly with vascular redistribution and pleural effusions. The distribution of the opacities is typically even and perihilar (central), prevalent in the middle and lower lung fields, and the vascular pedicle may be enlarged.

Noncardiogenic edema typically shows patchy peripheral or diffuse opacification of the lung fields, with air bronchograms and without cardiomegaly and pleural effusion; vascular pedicle is not enlarged. Septal lines, or Kerley lines, are more frequent in HPE, but may be present in noncardiogenic edema as well.

Unfortunately, these two types of edema frequently do not show up with the typical picture and may share many radiological features: in reality, the distinction becomes frequently impossible, besides the fact that they may coexist in the same patient (Desai 2002).

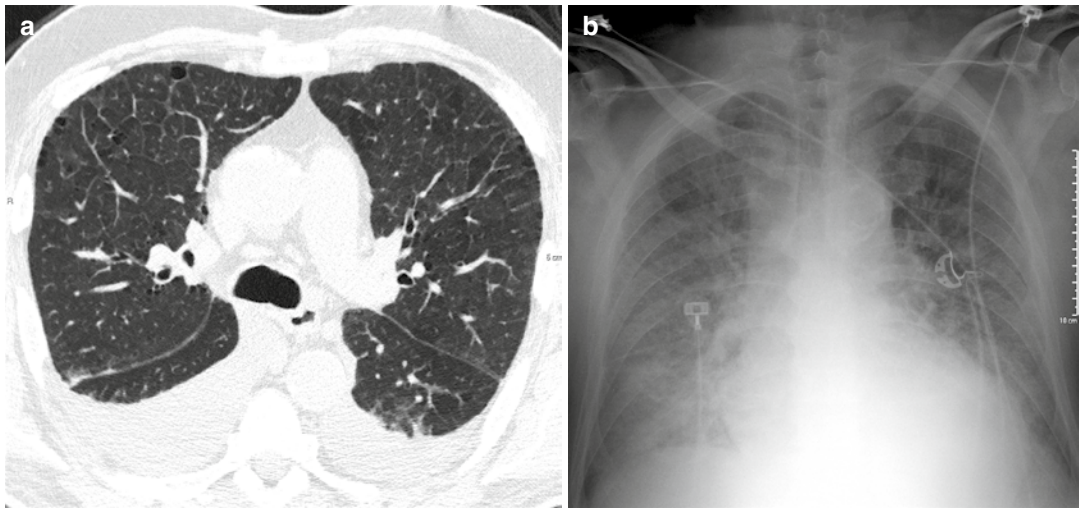

Fig. 22 Interstitial edema at HRCT. Presence of a bilateral diffuse septal pattern and mild bilateral pleural effusion (**a**). Corresponding chest X-ray picture (**b**)

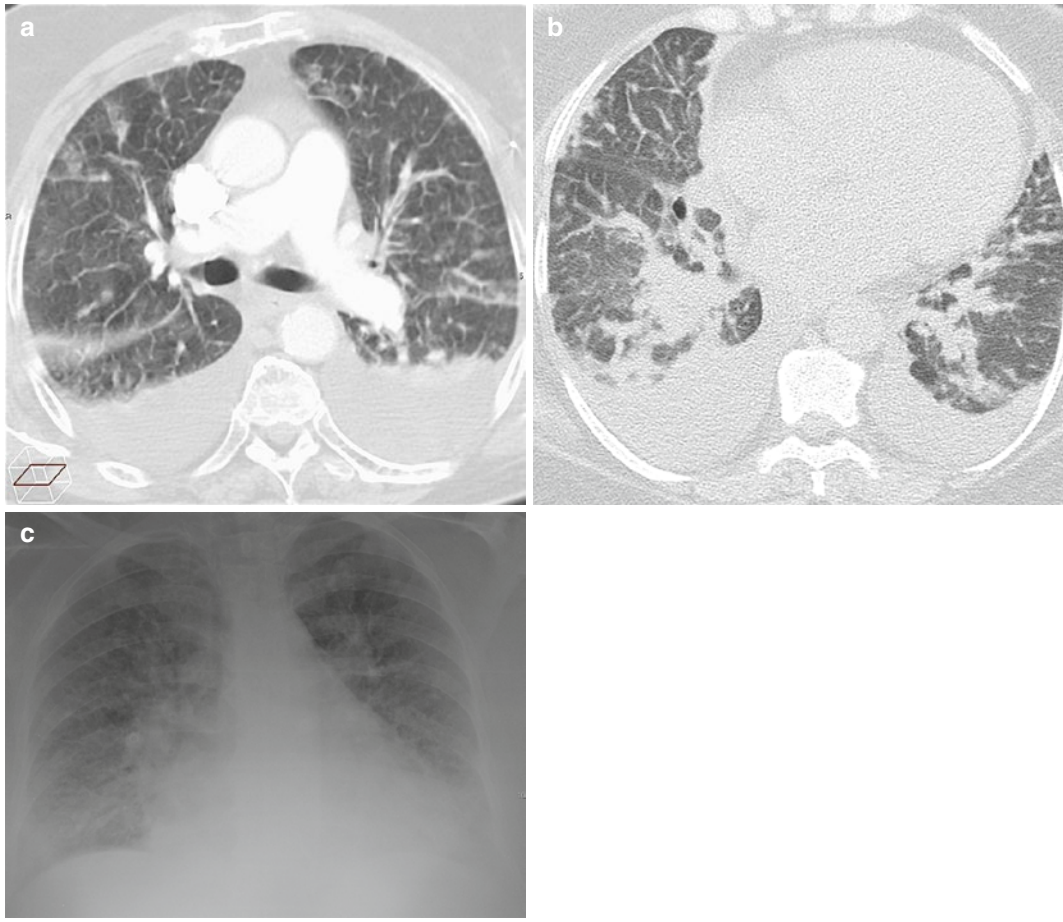

Fig. 23 HRCT findings in two cases of more advanced pulmonary edema. Extensive septal pattern, bronchial wall thickening, lobular ground-glass opacities and bilateral pleural effusion (**a**). Diffuse septal thickening, perihilar consolidations and bilateral pleural effusion (**b**); same patient of image (**b**); radiographic picture (**c**)

Furthermore, HPE has to be differentiated from several other conditions sharing a similar clinical and radiographic presentation, the so-called diffuse airspace disease. Those conditions, among others, are infective pneumonias, interstitial pneumonias, massive embolism, pulmonary hemorrhage, and aspiration (Ketai and Washington 2002).

Radiographic differentiation may be challenging and it is not always possible. HRCT may sometimes be very helpful and suggest the correct diagnosis, although in many cases it does not yield additional elements compared to chest X-ray (Ketai and Washington 2002; Rubinowitz et al. 2007).

The main HRCT finding in HPE is the septal pattern, with variable degrees of GGO. This HRCT pattern goes into differential diagnosis with several conditions, much rarer, such as pulmonary veno-occlusive disease (PVOD), lymphangitis carcinomatosis (although in this condition the septal thickening is usually nodular), sarcoidosis (which usually exhibit perilymphatic micronodules), Niemann-Pick disease, Erdheim Chester disease, cystic lymphangiectasia, lymphangiomyomatosis, and North American hantavirus infections (Oikonomou and Prassopoulos 2013).

6.6 Management and Treatment

Acute pulmonary edema is a life-threatening emergency. If necessary immediate intervention is required addressing the ABCs of resuscitation (airway, breathing, and circulation).

Subsequently, the therapy depends on the patient's condition and the cause of the pulmonary edema: measures may be aimed to preload reduction, afterload reduction, or inotropic support.

References

Aberle DR, Wiener-Kronish JP, Webb WR, Matthay MA (1988) Hydrostatic versus increased permeability pulmonary edema: diagnosis based on radiographic criteria in critically ill patients. Radiology 168(1):73–79

Akhtar S (2009) Fat embolism. Anesthesiol Clin 27(3): 533–550

Arakawa H, Kurihara Y, Nakajima Y (2000) Pulmonary fat embolism syndrome: CT findings in six patients. J Comput Assist Tomogr 24(1):24–29

ARDS Definition Task Force; Ranieri VM, Rubenfeld GD, Thompson BT, Ferguson ND, Caldwell E, Fan E, Camporota L, Slutsky AS (2012) Acute respiratory distress syndrome: the Berlin Definition. JAMA 307(23):2526–2533

Ashbaugh DG, Bigelow DB, Petty TL, Levine BE (1967) Acute respiratory distress in adults. Lancet 2(7511): 319–323

Barrera L, Mendoza F, Zuñiga J, Estrada A, Zamora AC, Melendro EI, Ramírez R, Pardo A, Selman M (2008) Functional diversity of T-cell subpopulations in subacute and chronic hypersensitivity pneumonitis. Am J Respir Crit Care Med 177:44–55

Bernard GR, Artigas A, Brigham KL et al (1994) The American-European Consensus Conference on ARDS: definitions, mechanisms, relevant outcomes, and clinical trial coordination. Am J Respir Crit Care Med 149(3 pt 1):818–824

Berrigan TJ Jr, Carsky EW, Heitzman ER (1966) Fat embolism. Roentgenographic pathologic correlation in 3 cases. Am J Roentgenol Radium Ther Nucl Med 96(4):967–971

Bolliger SA, Muehlematter K, Thali MJ, Ampanozi G (2011) Correlation of fat embolism severity and subcutaneous fatty tissue crushing and bone fractures. Int J Legal Med 125(3):453–458

Camus P, Fanton A, Bonniaud P, Camus C, Foucher P (2004a) Interstitial lung disease induced by drugs and radiation. Respiration 71(4):301–326

Camus P, Kudoh S, Ebina M (2004b) Interstitial lung disease associated with drug therapy. Br J Cancer 91(Suppl 2):S18–S23

Cardinale L, Priola AM, Moretti F, Volpicelli G (2014) Effectiveness of chest radiography, lung ultrasound and thoracic computed tomography in the diagnosis of congestive heart failure. World J Radiol 6(6):230–237

Castañer E, Alguersuari A, Gallardo X, Andreu M, Pallardó Y, Mata JM, Ramírez J (2010) When to suspect pulmonary vasculitis: radiologic and clinical clues. Radiographics 30(1):33–53

Castro CY (2006) ARDS and diffuse alveolar damage: a pathologist's perspective. Semin Thorac Cardiovasc Surg 18(1):13–19

Chong BJ, Kanne JP, Chung JH (2014) Headcheese sign. J Thorac Imaging 29(1):W13

Chung MP, Yi CA, Lee HY, Han J, Lee KS (2010) Imaging of pulmonary vasculitis. Radiology 255(2):322–341

Chung JH, Kradin RL, Greene RE, Shepard JA, Digumarthy SR (2011) CT predictors of mortality in pathology confirmed ARDS. Eur Radiol 21(4):730–737

Cleverley JR, Screaton NJ, Hiorns MP, Flint JD, Müller NL (2002) Drug-induced lung disease: high-resolution CT and histological findings. Clin Radiol 57(4):292–299

Colby TV, Fukuoka J, Ewaskow SP, Helmers R, Leslie KO (2001) Pathologic approach to pulmonary hemorrhage. Ann Diagn Pathol 5(5):309–319

Collard HR, Schwarz MI (2004) Diffuse alveolar hemorrhage. Clin Chest Med 25(3):583–592

Copetti R, Soldati G, Copetti P (2008) Chest sonography: a useful tool to differentiate acute cardiogenic pulmonary edema from acute respiratory distress syndrome. Cardiovasc Ultrasound 6:16

Cormier Y, Brown M, Worthy S, Racine G, Müller NL (2000) High-resolution computed tomographic characteristics in acute farmer's lung and in its follow-up. Eur Respir J 16(1):56–60

Cortese G, Nicali R, Placido R, Gariazzo G, Anrò P (2008) Radiological aspects of diffuse alveolar haemorrhage. Radiol Med 113(1):16–28

Curtis AM, Knowles GD, Putman CE, McLoud TC, Ravin CE, Smith GJ (1979) The three syndromes of fat embolism: pulmonary manifestations. Yale J Biol Med 52(2):149–157

Dakin J, Griffiths M (2002) The pulmonary physician in critical care 1: pulmonary investigations for acute respiratory failure. Thorax 57(1):79–85

Dalpiaz G, Maffessanti M (2013) Diffuse lung diseases. In: Geriatric imaging. Springer, Berlin/New York

Dalpiaz G, Nassetti C, Stasi G (2003) Diffuse alveolar haemorrhage from a rare primary renal-pulmonary syndrome: micropolyangiitis. Case report and differential diagnosis. Radiol Med 106(1–2):114–119

De Wever W, Meersschaert J, Coolen J, Verbeken E, Verschakelen JA (2011) The crazy-paving pattern: a radiological-pathological correlation. Insights Imaging 2(2):117–132

Desai SR (2002) Acute respiratory distress syndrome: imaging of the injured lung. Clin Radiol 57(1):8–17

Desai SR, Wells AU, Suntharalingam G et al (2001) Acute respiratory distress syndrome caused by pulmonary and extrapulmonary injury: a comparative CT study. Radiology 218:689–693

Dines DE, Burgher LW, Okakaki H (1975) The clinical and pathological correlation of fat embolism syndrome. Mayo Clin Proc 50:407–411

Elicker BM, Jones KD, Henry TS, Collard HR (2016) Multidisciplinary approach to hypersensitivity pneumonitis. J Thorac Imaging 31(2):92–103

Ely EW, Haponik EF (2002) Using the chest radiograph to determine intravascular volume status: the role of vascular pedicle width. Chest 121(3):942–950

Erasmus JJ, McAdams HP, Rossi SE (2002) High-resolution CT of drug-induced lung disease. Radiol Clin North Am 40(1):61–72

Feldman F, Ellis K, Green WM (1975) The fat embolism syndrome. Radiology 114(3):535–542

Ferguson ND, Fan E, Camporota L, Antonelli M, Anzueto A, Beale R, Brochard L, Brower R, Esteban A, Gattinoni L, Rhodes A, Slutsky AS, Vincent JL, Rubenfeld GD, Thompson BT, Ranieri VM (2012) The Berlin definition of ARDS: an expanded rationale, justification, and supplementary material. Intensive Care Med 38(10):1573–1582

Franquet T, Hansell DM, Senbanjo T, Remy-Jardin M, Müller NL (2003) Lung cysts in subacute hypersensitivity pneumonitis. J Comput Assist Tomogr 27(4): 475–478

Gallardo X, Castañer E, Mata JM, Rimola J, Branera J (2006) Nodular pattern at lung computed tomography in fat embolism syndrome: a helpful finding. J Comput Assist Tomogr 30(2):254–257

Gargani L, Volpicelli G (2014) How I do it: lung ultrasound. Cardiovasc Ultrasound 12:25

Gluecker T, Capasso P, Schnyder P, Gudinchet F, Schaller MD, Revelly JP, Chiolero R, Vock P, Wicky S (1999) Clinical and radiologic features of pulmonary edema. Radiographics 19(6):1507–1531

Goodman LR, Fumagalli R, Tagliabue P et al (1999) Adult respiratory distress syndrome due to pulmonary and extrapulmonary causes: CT, clinical, and functional correlations. Radiology 231:545–552

Greenberg HB (1968) Roentgenographic signs of post-traumatic fat embolism. JAMA 204(6):540–541

Gurd AR, Wilson RI (1974) The fat embolism syndrome. J Bone Joint Surg Br 56B(3):408–416

Han D, Lee KS, Franquet T, Müller NL, Kim TS, Kim H, Kwon OJ, Byun HS (2003) Thrombotic and non-thrombotic pulmonary arterial embolism: spectrum of imaging findings. Radiographics 23(6):1521–1539

Hanak V, Golbin JM, Ryu JH (2007) Causes and presenting features in 85 consecutive patients with hypersensitivity pneumonitis. Mayo Clin Proc 82:812–816

Heyneman LE, Müller NL (2000) Pulmonary nodules in early fat embolism syndrome: a case report. J Thorac Imaging 15(1):71–74

Ichikado K (2014) High-resolution computed tomography findings of acute respiratory distress syndrome, acute interstitial pneumonia, and acute exacerbation of idiopathic pulmonary fibrosis. Semin Ultrasound CT MR 35(1):39–46

Ichikawa Y, Kinoshita M, Koga T, Oizumi K, Fujimoto K, Hayabuchi N (1994) Lung cyst formation in lymphocytic interstitial pneumonia: CT features. J Comput Assist Tomogr 18:745–748

Janz TG, Madan R, Marini JJ, Summer WR, Meduri GU, Smith RM, Epler GR, Schnader J (2000) Clinical conference on management dilemmas: progressive infiltrates and respiratory failure. Chest 117(2):562–572

Jennette JC (2013) Overview of the 2012 revised International Chapel Hill Consensus Conference nomenclature of vasculitides. Clin Exp Nephrol 17(5):603–606

Kaewlai R, Avery LL, Asrani AV, Novelline RA (2008) Multidetector CT of blunt thoracic trauma. Radiographics 28(6):1555–1570

Ketai LH, Godwin JD (1998) A new view of pulmonary edema and acute respiratory distress syndrome. J Thorac Imaging 13(3):147–171

Ketai L, Washington L (2002) Radiology of acute diffuse lung disease in the immunocompetent host. Semin Roentgenol 37(1):25–36

Ketai L, Jordan K, Marom EM (2008) Imaging infection. Clin Chest Med 29(1):77–105

Kim M, Lee KY, Lee KW, Bae KT (2008) MDCT evaluation of foreign bodies and liquid aspiration pneumonia in adults. AJR Am J Roentgenol 190(4):907–915

Kliegerman SJ, Franks TJ, Galvin JR (2013) From the radiologic pathology archives: organization and fibrosis as a response to lung injury in diffuse alveolar damage, organizing pneumonia, and acute fibrinous and organizing pneumonia. Radiographics 33(7):1951–1975

Kokkarinen JI, Tukiainen HO, Terho EO (1992) Effect of corticosteroid treatment on the recovery of pulmonary function in farmer's lung. Am Rev Respir Dis 145:3–5

Komiya K, Ishii H, Murakami J et al (2013) Comparison of chest computed tomography features in the acute phase of cardiogenic pulmonary edema and acute respiratory distress syndrome on arrival at the emergency department. J Thorac Imaging 28(5):322–328

Kubo K, Azuma A, Kanazawa M, Kameda H, Kusumoto M, Genma A, Saijo Y, Sakai F, Sugiyama Y, Tatsumi K, Dohi M, Tokuda H, Hashimoto S, Hattori N, Hanaoka M, Fukuda Y, Japanese Respiratory Society Committee for formulation of Consensus statement for the diagnosis and treatment of drug-induced lung injuries (2013) Consensus statement for the diagnosis and treatment of drug-induced lung injuries. Respir Investig 51(4):260–277

Lara AR, Schwarz MI (2010) Diffuse alveolar hemorrhage. Chest 137(5):1164–1171

Lorente JA, Ballén-Barragán A, Herrero R, Esteban A (2015) Acute respiratory distress syndrome: does histology matter? Crit Care 19:337. doi:10.1186/s13054-015-1022-6

Maffessanti M, Dalpiaz G (2005) Diffuse lung diseases: clinical features, pathology HRCT. Springer, Milan/New York

Maffessanti M, Dalpiaz G (2011) Practical pulmonary pathology: a diagnostic approach. Elsevier, Philadelphia

Malagari K, Economopoulos N, Stoupis C et al (2003) High resolution CT findings in mild pulmonary fat embolism. Chest 123(4):1196–1201

Marten K, Schnyder P, Schirg E, Prokop M, Rummeny EJ, Engelke C (2005) Pattern-based differential diagnosis in pulmonary vasculitis using volumetric CT. AJR Am J Roentgenol 184(3):720–733

Mayberry JP, Primack SL, Müller NL (2000) Thoracic manifestations of systemic autoimmune diseases: radiographic and high-resolution CT findings. Radiographics 20(6):1623–1635

Meade MO, Cook RJ, Guyatt GH et al (2000) Interobserver variation in interpreting chest radiographs for the diag-

nosis of acute respiratory distress syndrome. Am J Respir Crit Care Med 161(1):85–90
Mellor A, Soni N (2001) Fat embolism. Anaesthesia 56(2):145–154
Miller WT Jr, Mickus TJ, Barbosa E Jr, Mullin C, Van Deerlin VM, Shiley KT (2011) CT of viral lower respiratory tract infections in adults: comparison among viral organisms and between viral and bacterial infections. AJR Am J Roentgenol 197(5):1088–1095
Milne EN (2010) Imaging expertise in critical care units. Radiology 256(3):1013
Milne EC, Pistolesi M (1994) Reading the chest radiograph: a physiologic approach. Mosby-Year Book, St Louis
Milne EN, Pistolesi M, Miniati M, Giuntini C (1985) The radiologic distinction of cardiogenic and noncardiogenic edema. AJR Am J Roentgenol 144(5):879–894
Mirka H, Ferda J, Baxa J (2012) Multidetector computed tomography of chest trauma: indications, technique and interpretation. Insights Imaging 3(5):433–449
Mönkäre S, Ikonen M, Haahtela T (1985) Radiologic findings in farmer's lung. Prognosis and correlation to lung function. Chest 87:460–466
Morgan PW, Goodman LR (1991) Pulmonary edema and adult respiratory distress syndrome. Radiol Clin North Am 29(5):943–963
Müller NL, White DA, Jiang H, Gemma A (2004) Diagnosis and management of drug-associated interstitial lung disease. Br J Cancer 91 Suppl 2:S24–S30
Murray JF (1975) Editorial: the adult respiratory distress syndrome (may it rest in peace). Am Rev Respir Dis 111(6):716–718
Nöbauer-Huhman IM, Eibenberger K, Schaefer-Prokop C et al (2001) Changes in lung parenchyma after acute respiratory distress syndrome (ARDS): assessment with high resolution computed tomography. Eur Radiol 11:2436–2443
Nucifora G, Hysko F, Vit A, Vasciaveo A (2007) Pulmonary fat embolism: common and unusual computed tomography findings. J Comput Assist Tomogr 31(5):806–807
Obadina ET, Torrealba JM, Kanne JP (2013) Acute pulmonary injury: high-resolution CT and histopathological spectrum. Br J Radiol 86(1027):20120614
Oikonomou A, Prassopoulos P (2013) Mimics in chest disease: interstitial opacities. Insights Imaging 4(1): 9–27
Park MS (2013) Diffuse alveolar hemorrhage. Tuberc Respir Dis (Seoul) 74(4):151–162
Piolanti M, Dalpiaz G, Scaglione M, Coniglio C, Miceli M, Violini S, Trisolini R, Barozzi L. Fat Embolism Syndrome: Lung Computed Tomography Findings in 18 Patients. J Comput Assist Tomogr. 2016 [Epub ahead of print] PubMed PMID: 26938691
Prasad R, Gupta P, Singh A, Goel N (2014) Drug induced pulmonary parenchymal disease. Drug Discov Ther 8(6):232–237
Primack SL, Miller RR, Müller NL (1995) Diffuse pulmonary hemorrhage: clinical, pathologic, and imaging features. AJR Am J Roentgenol 164(2):295–300
Ravenel JG, Heyneman LE, McAdams HP (2002) Computed tomography diagnosis of macroscopic pulmonary fat embolism. J Thorac Imaging 17(2): 154–156
Ribeiro CM, Marchiori E, Rodrigues R, Gasparetto E, Souza AS Jr, Escuissato D, Nobre LF, Zanetti G, de Araujo Neto C, Irion K (2006) Hydrostatic pulmonary edema: high-resolution computed tomography aspects. J Bras Pneumol 32(6):515–522
Richerson HB, Bernstein IL, Fink JN, Hunninghake GW, Novey HS, Reed CE, Salvaggio JE, Schuyler MR, Schwartz HJ, Stechschulte DJ (1989) Report of the Subcommittee on Hypersensitivity Pneumonitis. Guidelines for the clinical evaluation of hypersensitivity pneumonitis. J Allergy Clin Immunol 84:839–844
Rossi SE, Erasmus JJ, McAdams HP, Sporn TA, Goodman PC (2000) Cleverlay. Pulmonary drug toxicity: radiologic and pathologic manifestations. Radiographics 20(5):1245–1259
Rossi SE, Erasmus JJ, Volpacchio M, Franquet T, Castiglioni T, McAdams HP (2003) "Crazy-paving" pattern at thin-section CT of the lungs: radiologic-pathologic overview. Radiographics 23(6):1509–1519
Rubenfeld GD, Caldwell E, Granton JT, Hudson LD, Matthay MA (1999) Interobserver variability in applying a radiographic definition for ARDS. Chest 116(5): 1347–1353
Rubinowitz AN, Siegel MD, Tocino I (2007) Thoracic imaging in the ICU. Crit Care Clin 23(3):539–573
Schwarz MI, Albert RK (2004) "Imitators" of the ARDS: implications for diagnosis and treatment. Chest 125(4):1530–1535
Selman M (2011) Hypersensitivity pneumonitis. In: Schwarz M, King TE Jr (eds) Interstitial lung disease, 5th edn. People's Medical Publishing House-USA, Shelton, pp 597–625
Selman M, Pardo A, King TE Jr (2012) Hypersensitivity pneumonitis: insights in diagnosis and pathobiology. Am J Respir Crit Care Med 186(4):314–324
Sheard S, Rao P, Devaraj A (2012) Imaging of acute respiratory distress syndrome. Respir Care 57(4):607–612
Silva CI, Churg A, Müller NL (2007) Hypersensitivity pneumonitis: spectrum of high-resolution CT and pathologic findings. AJR Am J Roentgenol 188(2):334–344
Spagnolo P, Richeldi L, du Bois RM (2008) Environmental triggers and susceptibility factors in idiopathic granulomatous diseases. Semin Respir Crit Care Med 29:610–619
Spagnolo P, Rossi G, Cavazza A, Bonifazi M, Paladini I, Bonella F, Sverzellati N, Costabel U (2015) Hypersensitivity pneumonitis: a comprehensive review. J Investig Allergol Clin Immunol 25(4):237–250
Storto ML, Kee ST, Golden JA, Webb WR (1995) Hydrostatic pulmonary edema: high-resolution CT findings. AJR Am J Roentgenol 165(4):817–820
Svenningsen S, Nesse O, Finsen V, Hole A, Benum P (1987) Prevention of fat embolism syndrome in patients with femoral fractures – immediate or delayed operative fixation? Ann Chir Gynaecol 76(3):163–166

Talucci RC, Manning J, Lampard S, Bach A, Carrico CJ (1983) Early intramedullary nailing of femoral shaft fractures: a cause of fat embolism syndrome. Am J Surg 146(1):107–111

Thomeer MJ, Costabe U, Rizzato G, Poletti V, Demedts M (2001) Comparison of registries of interstitial lung diseases in three European countries. Eur Respir J Suppl 32:114s–118s

Tomiyama N, Müller NL, Johkoh T, Cleverley JR, Ellis SJ, Akira M, Ichikado K, Honda O, Mihara N, Kozuka T, Hamada S, Nakamura H (2001) Acute respiratory distress syndrome and acute interstitial pneumonia: comparison of thin-section CT findings. J Comput Assist Tomogr 25(1):28–33

Torrisi JM, Schwartz LH, Gollub MJ, Ginsberg MS, Bosl GJ, Hricak H (2011) CT findings of chemotherapy-induced toxicity: what radiologists need to know about the clinical and radiologic manifestations of chemotherapy toxicity. Radiology 258(1):41–56

Unger GF, Scanlon GT, Fink JN, Unger JB (1973) A radiologic approach to hypersensitivity pneumonias. Radiol Clin North Am 11(2):339–356

Vogelmeier C, Krombach F, Münzing S, König G, Mazur G, Beinert T, Fruhmann G (1993) Activation of blood neutrophils in acute episodes of farmer's lung. Am Rev Respir Dis 148:396–400

Ware LB, Matthay MA (2005) Clinical practice. Acute pulmonary edema. N Engl J Med 353(26): 2788–2796

Zompatori M, Calabrò E, Poletti V, Rabaiotti E, Piazza N, Viani S (2003) Hypersensitivity pneumonitis. High resolution CT findings with pathological correlations. A pictorial essay. Radiol Med 106(1–2):44–50